Ab Initio Studies of Silica-Based Clusters. Part I. Energies and Conformations of Simple Clusters

### J. C. G. Pereira,*,†,‡ C. R. A. Catlow,† and G. D. Price‡

The Royal Institution of Great Britain, 21 Albemarle Street, London W1X 4BS, United Kingdom, and Department of Geological Sciences, University College London, Gower Street, London WC1E 6BT, United Kingdom

To understand the complex mechanisms of reaction, solvation, and diffusion that determine the chemistry of silica in solution, it is necessary to study first the silicate clusters that participate in these processes. We have investigated, by ab initio density functional methods, all silica-based clusters of the form $Si_xO_y(OH)_z$, with a maximum of five silicon atoms and two intramolecular condensations, plus the six-silicon ring and the eight-silicon containing cube. In this article (part I), we report our results on the structure, charge distribution, and energy of the simpler clusters: the monomer $Si(OH)_4$, the dimer $Si_2O(OH)_6$, the linear trimer $Si_3O_2(OH)_8$, the ring trimer $Si_3O_3(OH)_6$, the linear tetramer $Si_4O_3(OH)_{10}$, the ring tetramer $Si_4O_4(OH)_8$, the linear pentamer $Si_5O_4(OH)_{12}$, and the cubic cage $Si_8O_{12}(OH)_8$. We also present density functional results for aluminosilicate clusters: $Al(OH)_4^-$, $Al_2O(OH)_6^{2-}$, and $SiAlO(OH)_6^-$. The results for the more complex clusters are presented in the subsequent article (part II). Our studies reveal a wide diversity of structures and consequently of charge distributions and energies for these clusters, that directly influence their chemical behavior, in particular the interaction with other clusters and with the solvent.

1. Introduction

There is no evidence that silica is soluble to any appreciable degree in any liquid other than water. The dissolution and deposition of silica in water involves chemical reactions of hydration and dehydration, generally described as:

$$(SiO_2)_n + 2H_2O \rightarrow (SiO_2)_{n-1} + Si(OH)_4$$
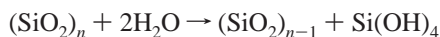
For nonporous amorphous silica, the equilibrium concentration of $Si(OH)_4$ at 25 °C corresponds to 70 ppm as SiO_2, the solubility of silica in water at this temperature. Most silica powders and gels, formed by extremely small particles of amorphous silica or by porous aggregates, with SiOH groups at the surface, exhibit a solubility of 100–130 ppm SiO_2.[1] Crystalline silica, like quartz, has a much lower solubility of ≈6 ppm SiO_2. The solubility of silica also increases steadily with pressure, temperature, and pH.

When silica has been dissolved previously in water at high temperature, pressure, or pH or when a solution containing a soluble silicate is hydrolyzed, supersaturated solutions of Si-(OH)$_4$ in pure water are formed. Silicon alkoxides, in particular $Si(OCH_3)_4$ (TMOS) and $Si(OCH_2CH_3)_4$ (TEOS), usually are used in sol–gel processing, to start the polymerization process:

$$Si(OR)_4 + 4H_2O \rightarrow Si(OH)_4 + 4ROH$$

These alkoxides are immiscible with water, and a solvent, typically an alcohol, is usually used to avoid liquid–liquid phase separation.

Monomeric silica comes out of supersaturated solutions in three ways: (1) as a deposit on a solid surface, where Si-(OH)$_4$ condenses with surface MOH groups and where M is a metal that forms a silicate at that pH; (2) as colloidal particles, remaining in suspension, if an insufficient area of a receptive solid surface is available to accept silica rapidly. These may aggregate, forming a silica gel, if the concentration of $Si(OH)_4$ is greater than 200–300 ppm,[1] or they may remain in solution, eventually forming opal. Very slow deposition may produce quartz.[3] (3) They may come out as biogenic amorphous silica, replicating exactly the detailed structure of organic forms, even after further crystallization, because the crystals are so small that even submicroscopic structures are retained.

Monomeric silicic acid, $Si(OH)_4$, has never been isolated in the gas phase, but it is soluble and stable in water, at 25 °C, for long periods, if the concentration is less than about 100 ppm as SiO_2.[1] When a solution of monomer is formed at a concentration greater than about 100–200 ppm (the solubility of amorphous silica), and in the absence of a solid phase on which the soluble silica might be deposited, the monomer polymerizes by condensation to form dimer and higher molecular weight species of silicic acid.

1.1. Experimental Studies. In the past 10 years, there have been extensive studies, using ^{29}Si NMR, liquid chromatography, vibrational spectroscopy, electron paramagnetic resonance (EPR), and other experimental techniques, of silica species in both gels and solutions.[2–8] ^{29}Si NMR spectroscopy proved to be particularly effective in identifying the concentration and gross structural features of such clusters.[9–14] Detailed reviews are given by Brinker and Scherer[15] and Hench and West.[16]

Kelts and Armstrong[13] were able to identify cyclic trimers in TEOS-based systems but not in those based on TMOS. When the water/alkoxide ratio decreases from 2/1 to 0.5/1 the cyclic trimer signal disappears. Kelts and Armstrong[13] explained these results, arguing that the probability of forming the 3-Si ring should increase with the number of hydroxyl groups available,

---

† The Royal Institution of Great Britain.
‡ University College London.

Energies and Conformations of Silica-Based Clusters

J. Phys. Chem. A, Vol. 103, No. 17, 1999 **3253**

which in turn should increase with the amount of water available. Cyclic trimers are formed preferentially in TEOS-based systems because the hydrolysis is much faster in TEOS- than in TMOS-based systems (unless the acid concentration is very low, as the growth mechanism is affected[13]).

However, partly because there are so many clusters simultaneously in solution, it is difficult to study their properties individually by experimental techniques, and we have little understanding of either the structural features of such clusters or of the energies and mechanisms of key condensation reactions. Recent developments in theoretical methods allow problems relating to molecular structures and energetics to be modeled with improved accuracy. It is the aim, therefore, of this and subsequent papers to investigate the fundamental aspects of silica clusters chemistry using a range of computational techniques.

In this article we concentrate on the conformations and energies in vacuo of key silica clusters, containing between one and eight Si atoms in vacuo. The smallest alumina clusters [$Al(OH)_4^-$, $Al_2O(OH)_6^{2-}$, and $AlSiO(OH)_6^-$] also have been analyzed and are reported here. Our calculations reveal a rich structural chemistry of such systems. Moreover, they provide the necessary basis for future studies of hydrated systems.

1.2. Previous Theoretical Studies. Several previous theoretical studies on silica clusters have been reported. Hartree−Fock (HF) results for $Si(OH)_4$ and $Si_2O(OH)_6$ are discussed in the review of Sauer.[17] The review of Heanry et al.[18] gives a detailed account of the Si−O bond in these systems. In another review, Gibbs and Boisen[19] show that molecular orbital calculations on molecules with first- and second-row cations (Na, Mg, Al, Si, P, S) yield bond lengths and angles that are close to those in chemically similar minerals. Bond lengths and angles in a crystal such as α-quartz can be reproduced with reasonable accuracy by MO calculations on a small molecule such as $Si_2O(OH)_6$.

Recent work on chains (dimer, trimer), rings (trimer, tetramer, pentamer, hexamer), and cages (prismatic hexamer, cubic octamer, hexagonal dodecamer) was reported by Hill and Sauer[20] and Moravetski et al.[21] HF studies for the monomer, the dimer, the four-silicon ring, and other silicate clusters were reported by Lasaga and Gibbs.[22,23] More recent density functional (DF) work on small silicate clusters was reported in ref 24.

The structure and possible decomposition routes for silanol, SiH_3OH, were discussed by Gordon and Pederson,[25] at the HF-MP2/6-31G(d,p) level of theory. The energies and structures of related molecules and radicals were also investigated. Ab initio calculations of the interaction of water with silanol were reported by Ugliengo et al.[26] at the MP2 level. The silanol dimer was not observed in the gas phase because of its readiness to yield disiloxane.[27] Ab initio techniques, using MP2 with symmetry constraints, were used to study the interaction of the silanediol molecule $SiH_2(OH)_2$ with H_2O and NH_3.[28] Several different conformations were investigated for $SiH_2(OH)_2$, $Si(OH)_4$, and $Si(OSiH_3)_2(OH)_2$. The differences in energy between these different conformations are always between 3.5 kJ mol^{-1} and 12 kJ mol^{-1}.

The lowest potential energy surface of disiloxane Si_2OH_6 was investigated by Luke,[29] as a function of two torsion angles H−Si−O−Si at the HF-MP2/631G(d,p) level of theory. Comparison between LDF and MP2 calculations for disiloxane and analogues, with Si substituted by Al, B, P, Ga, or Ge are presented by Stave and Nicholas[30] whereas these aluminosilicates were studied by Mortier et al.[31] and Brand et al.[32] at the HF/STO-3G level of theory. The first work aimed to explain the difference in properties of bridging and terminal silanol groups; the second to study the proton affinity of the central

bridging sites in Si−O−Al and Si−O−Si. The structures, force constants, and acidities of molecular structural analogues of disiloxane, $H_3T-O-TH_3$ and the protonated form $H_3T-OH-TH_3$, with T = Si, Al, B, and P, were calculated by Nicholas et al.[33] using restricted Hartree−Fock, with minimal, double- and triple-ζ basis functions.

A complete vibrational analysis of $Si_8O_{12}H_8$, including its 78 normal modes of vibration, was presented by Bornhauser and Calzaferri.[34] Its proposed structure, which is similar to that of $Si_8O_{12}(CH_3)_8$,[34] has a crown conformation for each of the face rings. Structural details, including bond lengths and bond angles, were also given in this study.

Self-consistent field (SCF) geometry optimizations for aluminosilicates, namely SiH_3OH, $Si(OH)_4$, and $Al(OH)_4^-$, were reported by Ahlrichs et al.[35] The substitution of silicon by aluminum in small clusters was studied recently by DF calculations.[24]

A comparison between HF and DF ab initio methods for molecular calculations was presented by Andzelm and Wimmer.[36] These authors found that DF calculations for equilibrium geometries, vibrational frequencies, bond dissociation energies, and reaction energies are closer to experimental data than HF results and that, although HF-optimized basis sets such as 6-31G** set can be used to obtain good geometries, the accurate prediction of reaction energies requires DF-optimized basis sets. Altmann et al.[37] found that DF bond lengths were slightly too long whereas HF bonds were slightly too short. For this author, in general, both methods seem to give similar geometrical parameters, although HF predictions might be more reliable. For Limtrakul and Tantanak,[38] DF and MP2 seem to provide results that are generally of comparable quality.

In our study we start by reporting the systematic analysis of all the silica clusters (containing only Si, O, and H) with a maximum of five silicon atoms, plus some relevant larger clusters, using ab initio density functional theory. This study depends critically on the cluster conformations, because of the strong intramolecular hydrogen bond interactions that exist in these molecules, so a careful conformation analysis was undertaken for each cluster. We calculated the energy differences between the most important conformations and the corresponding total condensation energies (i.e., the energy to form the cluster directly from the monomer), together with their structures and charge distributions.

2. Computational Details

The calculations reported in this article used the DF methodology and were undertaken with Dmol 2.1−96.0 from Molecular Simulations Inc.[39] In Dmol the atomic basis sets are defined numerically by a set of points (typically 300), from the origin to an outer distance of 5.3 Å (10 Bohr), each one described by a function of cubic spline coefficients, piecewise analytic, to generate first- and second-order energy derivatives. We used DN, DND, and DNP standard basis sets, plus enhanced ENP and triple TNP basis sets (see Appendix B).

Dmol generates a molecular grid in a spherical pattern around each atomic center, out to 5.3 Å, with a number of radial points typically given by $14(Z + 2)^{1/3}$,[39] where Z is the atomic number. These radial shells are logarithmically spaced to treat the rapid oscillations of the molecular orbitals near the nuclei. The angular points for each r shell increase with the quantum number l and are selected by schemes designed to yield exact angular integration, using quadrature methods and a product-Gauss rule in $\cos(\theta)$ and ϕ.[39] The total number of points per atom in the grid is approximately 1000. After generating the molecular grid, the program interpolates all the atomic quantities to this new

set of mesh points. To accelerate convergence far from the nucleus and to avoid integrating over the nucleus, a partition function is used.

In Dmol, the Coulombic potential $V_e(\vec{r})$ is calculated by solving the Poisson equation $-\nabla^2 V_e(\vec{r}) = 4\pi e^2 \rho(\vec{r})$, instead of integrating all over the space $V_e(\vec{r}) = \int \rho(\vec{r_i})/|\vec{r}-\vec{r_i}| \, d\vec{r_i}$. This approach, devised by Delley,[40] requires an analytical representation of the charge density. $\rho(\vec{r})$ is first partitioned in multipolar components $\rho_{\alpha lm}|(\vec{r}) - \vec{R}_\alpha)|$, which in turn are transformed into $V_{\alpha lm}$ components, whose sum gives the total Coulombic potential.[39]

The local exchange and correlation energies (BHL) are calculated separately, using the functional developed by von Barth and Hedin,[41] after Hedin and Lundqvist,[42] and reviewed by Moruzzi et al.,[43] for both spin-restricted and spin-unrestricted calculations. Nonlocal, gradient-corrected, exchange, and correlation contributions (BLYP) are calculated according to the functionals proposed respectively by Becke[44] and Lee et al.[45]

The following notation is widely used throughout this work: DF-BHL/DNP for DF with a von Berthe−Hedin−Lundqvist functional and a double basis set, DF-BLYP/DNP for DF with the same basis and a Becke−Lee−Yang−Parr functional, and DF-BLYP/TNP for DF with the same functional and a triple basis set. The monomer and the dimer are investigated using nonlocal density and a triple basis set (DF-BLYP/TNP); the trimers are studied with nonlocal DFT and a double basis set (DF-BLYP/DNP); larger clusters are analyzed at the LDA (local density approximation) level, with a double basis set (DF-BHL/DNP).

Unless explicitly stated otherwise, in Dmol calculations we used an SCF tolerance of 10^{-5} au for the electronic density, a gradient tolerance of 0.015 au for each coordinate, and a medium grid. We used spin-restricted calculations and no symmetry constraints were applied (point group C_1).

To save computer time, the most promising silica conformations were first studied using interatomic potential techniques, molecular dynamics, and energy minimization (Discover[46]). In some cases semiempirical methods (Mopac[47]) were also used. The selected geometries were then optimized fully with Dmol. At the end of each optimization, the Hessian matrix was checked to confirm that it was positive definite and that a true minimum had been found. Detailed information about specific optimization algorithms (implemented in codes as Dmol and Gaussian) can be found in Baker's work,[48,49] including determination of transition states[50] and constrained optimization techniques.[51,52] No Basis Set Superposition Errors (BSSE) or zero-point energy corrections were introduced.

3. Accuracy of the Results

We carried out a series of tests on small clusters, for which there are experimental and theoretical results available. We calculated the structure, charge distribution, and energies of Si-$(OH)_4$ and $Si_2O(OH)_6$ (presented in the results section), and of H_2O, H_2O-H_2O, OH^-, and H_3O^+ (shown in appendix A), using DF and HF methods, local and nonlocal functionals (DF-BHL and DF-BLYP), with different basis sets (DNP, ENP, TNP, and 6-31G**), SCF and gradient tolerances. HF tests on accuracy were done with Cadpac 5.1−6.0 from Cambridge University[53] using a 6-31G** Gaussian basis set, a second-order Møller−Plesset perturbation correction (MP2), a SCF tolerance of 10^{-7} au, and a gradient tolerance of 10^{-2} au. The knowledge thus acquired is essential to develop a critical understanding of the results obtained for the larger silica clusters. The tests show that it is already possible to predict the structure (bond lengths,

bond angles), the energies (hydrogen-bond energies, reactive energies), and in some cases even the charge distribution (electric dipoles), with high accuracy, using both HF and DF ab initio methods. Following our calculations, HF provides marginally better structural predictions than DF, but in compensation DF seems to predict slightly more accurate energies and is much faster than HF.

We found that accuracies as high as 0.02 Å, 2−3°, and 1−2 kcal mol^{-1} can be expected currently for ambitious but still affordable ab initio calculations for these systems. HF methods (at the MP2 level of theory) provide slightly better accuracy for structural data, but DF methods (at the nonlocal level of theory) appear to yield more reliable energies, and for larger systems they are the only ab initio technique that can be realistically applied.

LDA methods are much faster and describe well systems containing only primary bonds, but fail to predict correctly the main features of hydrogen-bonded systems. Although the description of primary covalent bonds depends essentially on the quality of the basis set, the description of hydrogen bonds depends primarily on the quality on the exchange and correlation functional.

Dmol calculations with nonlocal density (BLYP) require a better basis set. The SCF and geometry convergence are more problematic, and the overall treatment becomes much slower than in LDA calculations. However, with a large basis set it is a highly sophisticated method and very accurate structures and energies can be expected. In particular, it describes hydrogen bonds very well.

The electric dipole moment is highly sensitive to the method and basis set used, and for large molecules, very high levels of approximation are necessary to obtain reliable results.

4. Results

We now analyze the detailed energetic and structural information obtained from our calculations, presenting first our results for the monomer and dimer and discussing intramolecular effects that are relevant for all silica clusters. We present our results for the linear trimer, tetramer, and pentamer, discussing the cyclization effects responsible for the formation of ring structures. After that we also show our results for the trimer and tetramer ring, plus the octamer cubic cage, which have particularly relevant conformations. Finally, we discuss the results that we obtained for the smallest aluminum-containing anions.

All silica clusters discussed here are presented in Figures 1−8, including the most relevant energy, structure, and charge distribution information. For each cluster, there are three tables, for bond lengths, for bond angles, and for charges. The charges require 1 atom name (e.g., Si), the bond lengths require two atom names (e.g., Si−O) and the bond angles require three atom names (e.g., Si−O−Si). We simplified the notation for charges in the following way: (i) all charges start with 0, so we omit it. (ii) All oxygen charges are negative and all the other charges are positive, so we omit the sign of the charge (e.g., O 2938 indicates an oxygen charge of −0.2938 and Si 5257 indicates a Si charge of +0.5257). These assumptions make the tables much smaller and easier to read. Throughout this work, O_b and O_t denote bridging and terminal oxygen, respectively.

Tables 1-4 contain the most important data for the silica monomer, the silica dimer and the aluminosilicate clusters. The total energy for all silica clusters discussed in this work is presented in Table 5. For each cluster, the different conformations are ordered by their energies. The condensation energy to

Energies and Conformations of Silica-Based Clusters

J. Phys. Chem. A, Vol. 103, No. 17, 1999 **3255**

TABLE 1: Total Energy (Hartree), Bond Lengths (Å), Bond Angles, and Charge Distribution for Isolated Si(OH)$_4$ Molecule

| | | | | | bond angle | |
| | | | bond length | | O–Si–O– | |
method	total energy	SiO	OH	O--H	(4×,2×)	Si–O–H
BHL/DNP	−589.89392	1.64	0.99	2.68	105.6, 117.6	112.4
ENP	−589.92865	1.63	0.97	2.73	106.1, 116.5	115.5
BLYP/DNP	−593.09657	1.67	0.99	2.71	105.7, 117.4	111.1
ENP	−593.13341	1.66	0.97	2.78	106.5, 115.6	116.2
TNP	−593.14211	1.65	0.97	2.78	106.6, 115.4	116.5
MP2/6-31G**	−591.76320	1.647	0.960		106.4, 115.9	114.9
ref[17] (HF)		1.626	0.942		106.6, 115.4	118.8

| | Hirshfeld | | | Mulliken | | |
	Si	O	H	Si	O	H
BHL/DNP	0.4473	−0.2842	0.1724	0.8660	−0.7620	0.5460
ENP	0.4598	−0.2887	0.1738	0.5590	−0.3530	0.2130
BLYP/DNP	0.5087	−0.2885	0.1613	1.1510	−0.8090	0.5220
ENP	0.5215	−0.2940	0.1637	0.9130	−0.3830	0.1550
TNP	0.5267	−0.2962	0.1645	1.8220	−0.6000	0.1430
MP2/6-31G**				1.2320	−0.6593	0.3512

TABLE 2: Total Energy (Hartree), Bond Lengths (Å), Bond Angles, Electric Dipole (Debye), and Charge Distribution for an Isolated Si$_2$O(OH)$_6$ Molecule (t = Terminal, b = Bridging)

| | Si$_2$O(OH)$_6$ | | |
	BHL/DNP	BLYP/DNP	TNP
energy	−1103.8924	−1109.7564	−1109.8323
length			
SiO$_b$	1.65	1.67	1.65
SiO$_t$	1.65	1.66−1.68	1.64−1.66
OH	0.99	0.98−0.99	0.97
O--H (2×)	1.91	2.20	2.52
O--H (2×)	2.98	3.07	2.94
O--H (2×)	2.84	2.83	2.81
angle			
Si–O–Si	118.4	123.1	132.1
O–Si–O	105.9−108.3	107.1−112.9	107.8−113.7
Si–O–H	111.8	108.7−113.4	114.1−117.7
OH--H	146.8−147.4	144.4−145.2	134.8−138.0
Hirshfeld			
Si	0.4598	0.5199	0.5367
O$_b$	−0.2776	−0.2982	−0.3036
O$_t$	−0.2691	−0.2796	−0.2902
H	0.1621	0.1560	0.1619
Mulliken			
Si	0.9785	1.2410	1.7615
O$_b$	−0.5800	−0.7070	−0.8260
O$_t$	−0.7742	−0.8178	−0.6006
H	0.5447	0.5223	0.1511
dipole	1.09	1.32	0.85

TABLE 3: Si(OH)$_4$ Condensation Energy (kcal mol^{-1}) after Local DF-BHL and Nonlocal DF-BLYP and HF-MP2 Optimizations, Compared with HF-MP2/6-31G Reference Value, Using Numerical (DN, DND, DNP, TNP) Basis Sets**

method	condensation energy
BHL/DNP	−9.38
BLYP/DNP	−2.84
TNP	−2.22
ref[62] (HF)	−7.8

form each cluster from the monomer is presented in Table 6, for the lowest conformations only. Calculated and corrected energies (subtracting 3.3 kcal mol^{-1} per H-bond when O−H < 1.85 Å, as discussed below), are reported. The same values, divided by the number (n) of condensation reactions to form the cluster and by the number (s) of silicon atoms in the cluster are also presented. Silica clusters are classified in this work

TABLE 4: Total Energy (Hartree), Bond Lengths (Å), Bond Angles, Electric Dipole (Debye), and Hirshfeld Charges for Isolated Al(OH)$_4^-$, Al$_2$O(OH)$_6^{2-}$, and AlSiO(OH)$_6^-$ Clusters^a

	Al(OH)$_4^-$	Al$_2$O(OH)$_6^{2-}$	AlSiO(OH)$_6^-$
energy	−543.00884	−1010.0090	−1057.0357
length			
AlO$_b$		1.75	1.79
SiO$_b$			1.62
AlO$_t$	1.78−1.79−1.81d	1.75−1.81d	1.75−1.81d
SiO$_t$			1.65−1.68d
OH$_t$	0.98	0.98−1.01a	0.98−1.05a
O- -H		1.89−1.93	1.55$_{dAl}$−2.21$_{dSi}$
angle			
AlOAl		112.0	
AlOSi			115.0
OAlO	106.2−116.2	103.7−109.8	109.4−114.2
O−Si−O			103.9−109.6
AlOH	108.5	99.0−102.5	105.0−106.2
Si−O−H			104.4−106.2
Hirshfeld			
O$_b$		−0.4730	−0.3635
Al	0.3082	0.2928	0.3733
Si			0.3920
O$_{tAl}$	−0.4199	−0.3821	−0.3987
O$_{dAl}$		−0.4478	−0.3190
O$_{aAl}$		−0.4307	−0.4160
H$_{tAl}$	0.0928	0.0764	0.1095
H$_{dAl}$		0.0848	0.1277
H$_{aAl}$		0.0432	0.0775
O$_{tSi}$			−0.3116
O$_{dSi}$			−0.2864
O$_{aSi}$			−0.3470
H$_{tSi}$			0.1462
H$_{dSi}$			0.1453
H$_{aSi}$			0.0703
dipole	0.00	41.1	32.8

^{a} Key: d = H-bond donor group; a = H-bond acceptor group; t = terminal group not involved in H-bonds. The heavy atom to which the hydroxyl group is attached is also indicated.

according to the NMR notation, Q_n^m, where n represents the number of silicons that are bonded to m bridging oxygens.

4.1. Intramolecular Effects: Monomer and Dimer. *4.1.1. Energy and Conformations. Monomer.* In Si(OH)$_4$, two conformations need to be considered, with point symmetry D_2d and S_4. The S_4 conformation is the global minimum in the gas phase. The structure and charge distribution for both conformations are presented in Figure 1, for the more accurate calculations (DF-BLYP/TNP level).

With local density and a double basis set, at the DF-BHL/DNP level of approximation, the energy difference between these conformations is only 1.0 kcal mol^{-1}. At the much higher DF-BLYP/TNP level of approximation, with nonlocal density and a triple basis set, the energy difference increases to 1.8 kcal mol^{-1}. For the same energy barrier, Sauer[17] reported a slightly higher value, at the HF-MP2/6-31G** level: 3.2 kcal mol^{-1}. The charges in the S_4 conformation are slightly larger, but the dipole is smaller. These differences, although very small, should be significant, given the simplicity of the cluster.

Dimer. Disilicic acid, Si$_2$O(OH)$_6$, is the first product of silica condensation, probably the most important reaction in silica cluster chemistry. The structure and charge distribution for the conformations with the lowest energy and the highest symmetry, C_2 and C_{2v}, respectively, are presented in Figure 2, for the more accurate calculations (DF-BLYP/TNP level). At the DF-BHL/DNP level of approximation, the C_2 conformation is +11.0 kcal mol^{-1} more stable than the C_{2v} conformation, whereas at the DF-BLYP/TNP level the difference decreases to +5.7 kcal mol^{-1}.

These energy differences are substantial, even for the more sophisticated level of approximation, and show the importance

TABLE 5: Total Energy/Hartree (1 Ha = 627.51 kcal mol^{-1} for Different Conformations (Ordered by Decreasing Energy) of Several Silicate Clusters, Optimized at the DF-BHL/DNP, DF-BLYP/DNP, and DF-BLYP/TNP Levels of Approximation

		total energy		
		BHL-DNP	BLYP/DNP	BLYP/TNP
	H_2O	−75.910391	−76.441266	−76.455469
.	Q_1^0	−589.89232 −589.89392		−593.13921 −593.14211
—	Q_2^1	−1103.8749 −1103.8924		−1109.8232 −1109.8323
∧	$Q_2^1 Q_1^2$	−1617.8857 −1617.8905	−1626.4160 −1626.4195	
∧∧	$Q_2^2 Q_2^1$	−2131.8869 −2131.9053		
∨∨	$Q_3^2 Q_2^1$	−2645.7894 −2645.8975		
△	Q_3^2	−1541.9434 −1541.9447 −1541.9532	−1549.9572	
□	Q_4^2	−2055.9243 −2055.9751		
▱	Q_8^3	−3808.2177 −3808.2202		

TABLE 6: Total Condensation Energy (kcal mol^{-1}) for Optimized Silicate Clusters[a]

		condensation energy		
		CE (CE$_c$)	CE (CE$_c$)/n	CE (CE$_c$)/s
—	Q_2^1	−9.4 (−2.8)	−9.4 (−2.8)	−4.7 (−1.4)
∧	$Q_2^1 Q_1^2$	−18.5 (−11.9)	−9.3 (−6.0)	−6.2 (−4.0)
∧∧	$Q_2^2 Q_2^1$	−38.2 (−21.7)	−12.7 (−7.2)	−9.5 (−5.4)
∨∨	$Q_3^2 Q_2^1$	+6.4 (+6.4)	+1.3 (+1.3)	+1.6 (+1.6)
△	Q_3^2	−1.6 (−1.6)	−0.5 (−0.5)	−0.5 (−0.5)
△ □	Q_4^2	−25.7 (−12.5)	−6.4 (−3.1)	−6.4 (−3.1)
▱	Q_8^3	+4.1 (+4.1)	+0.3 (+0.3)	+0.5 (+0.5)

[a] CE = calculated; CE$_c$ = corrected with 3.3 kcal mol^{-1} per H-bond when O- -H > 1.85 Å (see text); n = number of condensation reactions to form the cluster; s = number of silicons in the cluster.

of these conformational analyses. The type of reaction undergone by a given cluster depends considerably on its conformations; and although no bond breaking is needed to transform one conformation into another, such energy barriers will be significant, particularly at low temperatures.

The charges in the C_2 conformation are influenced by the oxygen−hydrogen interactions, although these are expected to be weak, considering the large O- -H distances and the small hydrogen bond energies. Oxygen and hydrogen atoms in donor hydroxyl groups have more positive charges, whereas the opposite is observed in acceptor hydroxyl groups, which indicates some real charge transfer from the donor groups to the acceptors. In the C_{2v} conformation, the two terminal oxygens in the chain ends have more negative charges than the other four.

Si **5257**	SiO_b	$SiOSi$
O_b	SiO_t **1.66**	$O_b SiO_b$
O_t **2938**	OH **0.97**	$O_t SiO_t$ **103.2-112.7**
H **1625**	$O\text{-}H$	$SiOH$ **114.6**
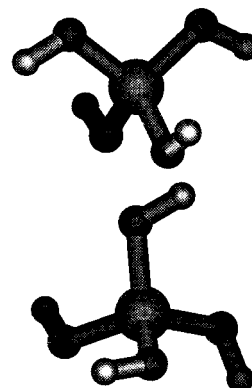
Si **5271**	SiO_b	$SiOSi$
O_b	SiO_t **1.65**	$O_b SiO_b$
O_t **2968**	OH **0.97**	$O_t SiO_t$ **106.6-115.4**
H **1650**	$O\text{-}H$	$SiOH$ **116.5**

Figure 1. Bond lengths (Å), bond angles (degrees), and Hirshfeld atomic charges (0. and minus sign in O charges are omitted) for D_2d and S_4 Si(OH)$_4$ conformations, optimized at the DF-BLYP/TNP level of approximation. Energy difference: $D_2d \rightarrow S_4$ $E = -1.8$ kcal mol^{-1}.

Si **5343**	SiO_b **1.65**	$SiOSi$ **136.6**
O_b **3030**	SiO_t **1.65-1.66**	$O_b SiO_b$
O_t **2863-3030**	OH **0.97**	$O_t SiO_t$ **103.2-112.7**
H **1607-1628**	$O\text{-}H$	$SiOH$ **113.8-116.2**
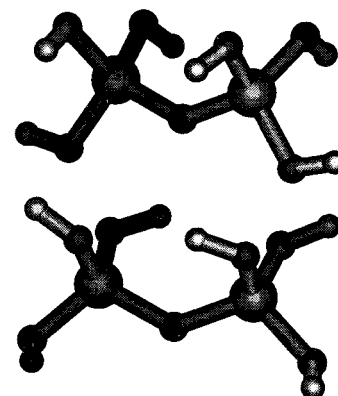
Si **5368**	SiO_b **1.65**	$SiOSi$ **132.1**
O_b **3036**	SiO_t **1.64-1.66**	$O_b SiO_b$
O_t **2837-3036**	OH **0.97**	$O_t SiO_t$ **107.8-113.7**
H **1490-1687**	$O\text{-}H$ **2.52**	$SiOH$ **114.1-117.7**

Figure 2. Bond lengths (Å), bond angles (degrees), and Hirshfeld atomic charges (0. and minus sign in O charges are omitted) for C_{2v} and C_2 Si$_2$O(OH)$_6$ conformations, optimized at the DF-BLYP/TNP level of approximation. Energy difference: $C_{2v} \rightarrow C_2$ $E = -5.7$ kcal mol^{-1}. Dipole moment: $\mu = 1.60$ D (C_{2v}) and $\mu = 0.85$ D (C_2).

The electric dipole moment is highly sensitive to the method used (in part, because of the Si−O−Si angle), changing from 1.32 D to 0.85 D when a triple instead of a double basis set is used, and from 1.09 D to 1.32 D when nonlocal exchange and correlation energies are added (C_2 conformation). In this respect, even the value obtained with nonlocal corrections and triple

basis set might be not considered as totally reliable. The electric dipole in the monomer is zero because of its symmetry.

The condensation energy to form the dimer from the monomer ($2Si(OH)_4 + \Delta E \rightarrow Si_2O(OH)_6 + H_2O$), for the lowest energy conformations and the levels of theory investigated so far, is presented in Table 3. Within the LDA, the condensation energy is relatively large, -9.4 kcal mol^{-1}, and almost equal for all the basis sets tested. The condensation energy drops considerably, however, at the DF-BLYP/DNP level (i.e., a nonlocal density), calculated as -2.8 kcal mol^{-1}. This finding is to be expected because of the two hydrogen bonds present in $Si_2O(OH)_6$, which are not present in the $Si(OH)_4$ reactants. When a triple basis set is applied, the energy decreases even further to -2.2 kcal mol^{-1}, which we expect to be an accurate prediction for the energy of this reaction.

These results closely resemble the trends observed for the hydrogen bond energy in the water dimer (H_2O-H_2O) presented in Table 8 (see Appendix A). As in the water dimer, the MP2 prediction (-7.8 kcal mol^{-1}) is less than the local DF-BHL/DNP, but more than the best nonlocal DF-BLYP/TNP. Assuming that the difference in energy between local and nonlocal density calculations is due only to the two intramolecular hydrogen bonds occurring in $Si_2O(OH)_6$, the error per hydrogen bond in the local density calculations can be estimated as about -3.3 kcal mol^{-1}, which is reasonably close to the corresponding error of -4.7 kcal mol^{-1} in the water dimer. The difference between the two values is probably attributable to the Si$-$O$-$Si angle requirements, which force the hydrogen bonds to be 0.2 Å longer, and consequently weaker, than in the water dimer, for the same level of approximation.

4.1.2. Structures. Monomer. Monosilicic acid, $Si(OH)_4$, is a fundamental molecule in Si chemistry, particularly in sol$-$gel and zeolite synthesis. However, because it is very unstable in the gas phase, no experimental data are available for the isolated molecule. The results presented in Table 1 for the S_4 conformation, using DF-BHL/DNP and DF-BLYP/TNP levels of approximation, are therefore compared with published HF calculations.

The LDA method with polarization functions (DF/BHL/DNP) predicts well the two O$-$SI$-$O angles in the monomer, one occurring four times (105.6°) and the other twice (117.6°), in reasonable agreement with HF values (106.6° and 115.4°).[17] The O$-$H and Si$-$O bond lengths, however, are 0.05 and 0.02 Å longer than the reference values, respectively. The calculated Si$-$O$-$H angle (112.4°) is also relatively far from the reference result (118.8°). At this level of approximation, the accuracy still depends very much on the quality of the atomic basis set; using an enhanced basis set, with the same basis functions for Si, but using a triple basis set to describe the oxygens and hydrogens (DF-BHL/ENP) results in a considerable improvement in the Si$-$O and O$-$H bond lengths (1.63 Å and 0.97 Å), and also in the O$-$Si$-$O (106.1° and 116.5°) and Si$-$O$-$H (115.5°) angles. These values are very close to the results in ref 17, showing that LDA can describe the structure of a given molecular system with very high accuracy when no hydrogen bonds are present and a good basis set is used.

At the DF-BLYP/DNP level, with nonlocal density, the O$-$H bond length and the O$-$Si$-$O angles are the same as the DF-BHL/DNP values, with the same basis set, but the Si$-$O bond length and the Si$-$O$-$H bond angle become less accurate: 1.67 Å and 111.1°. DFT tends slightly to overestimate the bond lengths, and this feature seems to be enhanced by the introduction of nonlocal corrections. To increase the quality of the results

obtained for structural properties and to regain the previous accuracy, a much better basis set is necessary.

The overall structural description improves substantially with use of an enhanced basis set (DF-BLYP/ENP). The Si$-$O and O$-$H bond lengths decrease to 1.66 Å and 0.97 Å, and both O$-$Si$-$O bond angles, 106.5° and 115.6°, match the values in ref 17. In particular, the Si$-$O$-$H angle improves considerably to 116.2°. A further refinement, introducing five additional basis functions for silicon to obtain what is essentially a triple basis set for all atoms, leads again to an improvement of the results obtained, which are now very close to the HF values reported in ref 17. The O$-$Si$-$O angles match exactly the reference values, the Si$-$O$-$H angle is 2.3° smaller and the Si$-$O and O$-$H bond lengths are only 0.02 Å and 0.03 Å larger, respectively.

The distance between adjacent hydroxyl groups is clearly too large in this cluster to allow the formation of hydrogen bonds. Consequently, no important differences were found between local DF-BHL and nonlocal DF-BLYP methods. For a double basis set, the O- -H distance is calculated as 2.68$-$2.69 Å with local DFT and 2.71 Å for a nonlocal calculation, whereas these values increased slightly to 2.73 Å and 2.78 Å, respectively, with the enhanced basis set. The latter is also the value predicted at the highest DF-BLYP/TNP level of approximation.

In the D_2d monomer conformation, at the DF-BLYP/TNP level, the Si$-$O bond length is slightly longer and the O$-$Si$-$O and Si$-$O$-$H angles are slightly smaller.

Dimer. The situation changes completely in the silicate dimer, in which hydrogen bonds do play a very important role. The corresponding results are presented in Table 2, for the lowest energy C_2 conformation.

In the less ambitious $Si_2O(OH)_6$ calculation at the (DF-BHL/DP) level, the O- -H and O- -O distances between the two hydroxyl groups on each side of the Si$-$O$-$Si plane are only 0.06$-$0.07 Å smaller than in the hydrogen bond in the gas-phase water dimer (see Appendix A). However, the O- -H distances increase considerably to 2.20 Å at the DF-BLYP/DNP level, with nonlocal corrections for exchange and correlation energies. The O- -H distances increase even more at the DF-BLYP/TNP level to 2.52 Å, which is already at the limit of what can be expected for a hydrogen bond distance. The O$-$H$-$O angle is between 134.8° and 147.4° for all calculations, very far therefore from the equivalent angle in the water dimer.

These differences between the results for local and nonlocal levels of approximation suggest that, as in the water dimer, the LDA is overestimating the strength of the hydrogen bonds. Although, for the water dimer, a pure hydrogen bond depends much more on the charge distribution than on the basis set, in this cluster the two O- -H distances are closely related to the Si$-$O$-$Si angle, which depends very much on the quality of the basis set used. The values obtained for these parameters are thus the result of the combination of the charge distribution in the O- -H distances and the atomic basis set in the Si$-$O$-$Si angle.

In the LDA calculations, the overestimated O- -H interactions between the two parts of the dimer force the Si$-$O$-$Si angle to decrease to 118.1°. With nonlocal DFs, the angle increases progressively to 123.1° (DF-BLYP/DNP), and finally 132.1°, in the best calculation (DF-BLYP/TNP). This last value is expected to be a very accurate and reliable result, considering the excellent agreement with experimental and theoretical data obtained for the previous systems at this sophisticated level of approximation. The other four possible O- -H interactions, grouped in two pairs disposed diagonally, are too large (2.94

Å and 2.81 Å in the best calculation) to have any significant hydrogen-bonding character.

At the DF-BHL/DNP level of approximation, the Si—O bond becomes very accurate, 1.65 Å, but the Si—OH angle is too small, 111.8°. As for the monomer, nonlocal exchange and correlation corrections again increase the Si—O bonds (to 1.66–1.68 Å), and only when the triple basis set is used, the overall accuracy improves significantly: the Si—O and O—H bond lengths decrease to 1.65 Å and 0.97 Å, whereas the Si—O—H bond angle increases to 114.1–117.7°. Although no experimental results are available for $Si_2O(OH)_6$, following the results for $Si(OH)_4$ and H_2O- -H_2O, the Si—O and O—H bond lengths are probably only 0.02–0.03 Å smaller than those calculated here, whereas the Si—OH angle is probably about 119°, 3° larger than the average value calculated here.

At the DF-BLYP/TNP level of approximation, the bond lengths are equal in both C_2 and C_{2v} dimer conformations. The Si—O—Si angle is larger in the C_{2v} conformation, and the O—Si—O and Si—OH angles are slightly smaller.
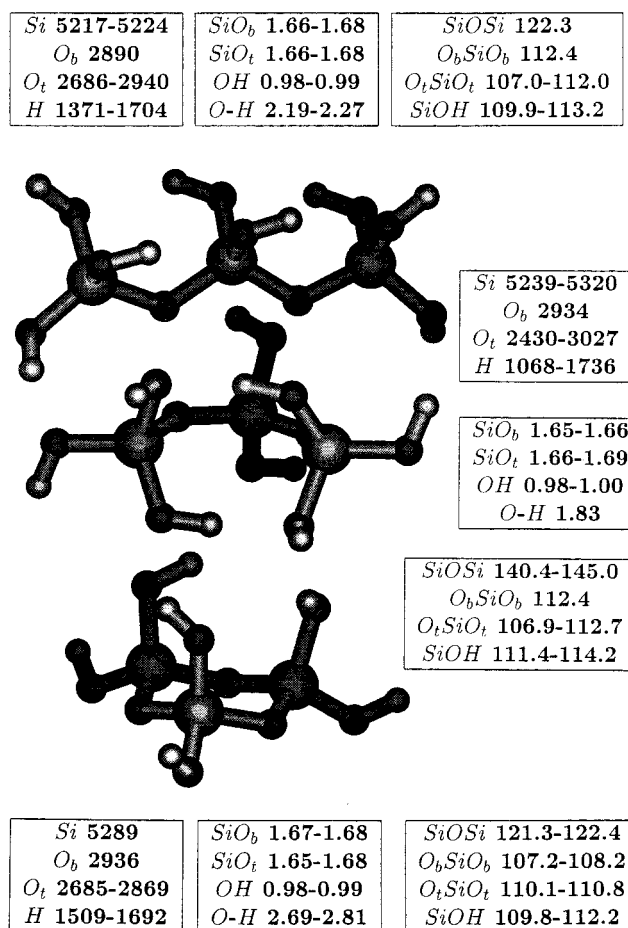
4.2. Effects of Ring Formation: Linear Trimer, Tetramer, and Pentamer. *4.2.1. Energy and Conformations. Linear Trimer.* The linear trimer and the trimer ring are the largest silicate clusters studied in this work with nonlocal DFs. The comparison between the results obtained for DF-BHL/DNP and DF-BLYP/DNP levels of approximation is valuable, therefore, because it helps us to estimate the accuracy of the results obtained for the larger clusters, where only DF-BHL/DNP calculations were possible.

At the DF-BHL/DNP level of approximation, the lowest energy conformation found for the linear trimer is almost cyclic, with two hydrogen bonds closing the ring. This conformation is 3.0 kcal mol^{-1} more stable than the straight one, where the chain ends are far apart. The structure and charge distribution for both conformations are shown in Figure 3, for the more accurate calculations (DF-BLYP/DNP). At the DF-BLYP/DNP level (including nonlocal exchange and correlation), the difference in energy between these conformations decreases only slightly to 2.2 kcal mol^{-1}.

The almost cyclic conformation may, in turn, be transformed into the trimer ring by a intramolecular condensation reaction. The corresponding energy, although positive, is sufficiently small (+16.9 kcal mol^{-1} at the DF-BHL/DNP level and +13.2 kcal mol^{-1} at the DF-BLYP/DNP level) to explain how a relatively strained cluster such as the three-silicon ring may be formed.

The hydrogen bonds are overestimated at the DF-BHL/DNP level of approximation, because the O- -H bond lengths are too small (≈1.64 Å) and the O—H bond lengths in the acceptor groups are too large (1.02 Å). The total condensation energy is consequently too high (−18.5 kcal mol^{-1}) when compared with the best results obtained for the dimer. With application of the energy difference between local and nonlocal DF found for the dimer (3.3 kcal mol^{-1} per hydrogen bond), the corrected condensation energy is calculated as −11.9 kcal mol^{-1}, which seems more reasonable, considering the results for the dimer.

At the DF-BLYP/DNP level of approximation, the condensation energy becomes −7.7 kcal mol^{-1}, smaller than even the corrected DF-BHL/DNP value. For larger clusters with hydrogen bonds, which at the moment can only be studied at the DF-BHL/DNP level of approximation, the calculated condensation energies should therefore be overestimated and even the corrected values should be considered as a crude upper limit for the correct results. This effect is due to the increasing number of weak interactions developed in these larger clusters, which

Si 5217-5224	SiO_b 1.66-1.68	$SiOSi$ 122.3
O_b 2890	SiO_t 1.66-1.68	O_bSiO_b 112.4
O_t 2686-2940	OH 0.98-0.99	O_tSiO_t 107.0-112.0
H 1371-1704	O-H 2.19-2.27	$SiOH$ 109.9-113.2

Si 5239-5320
O_b 2934
O_t 2430-3027
H 1068-1736

SiO_b 1.65-1.66
SiO_t 1.66-1.69
OH 0.98-1.00
O-H 1.83

$SiOSi$ 140.4-145.0
O_bSiO_b 112.4
O_tSiO_t 106.9-112.7
$SiOH$ 111.4-114.2

Si 5289	SiO_b 1.67-1.68	$SiOSi$ 121.3-122.4
O_b 2936	SiO_t 1.65-1.68	O_bSiO_b 107.2-108.2
O_t 2685-2869	OH 0.98-0.99	O_tSiO_t 110.1-110.8
H 1509-1692	O-H 2.69-2.81	$SiOH$ 109.8-112.2

Figure 3. Bond lengths (Å), bond angles (degrees), and Hirschfeld atomic charges (0. and minus sign in O charges are omitted) for Si_3O_2-$(OH)_8$ conformations forming $Si_3O_3(OH)_6$, optimized at the DF-BLYP/DNP level of approximation. Energy difference: (top) → (medium) E = −2.2 kcal mol^{-1}; (medium) → (below) E = +13.2 kcal/mol. Dipole moment: μ = 1.55 D (above), μ = 0.36 D (center), and μ = 3.2 D (bottom).

are overestimated in local density calculations but are too small to be corrected.

At the DF-LYP/DNP level, the O- -H and O—H bond lengths (1.83 Å and 1.00 Å, respectively), are close to the expected values. However, because nonlocal density calculations tend to overestimate the bond lengths, the correct Si—O bond lengths, in particular, should be roughly 0.04 Å shorter than those calculated here. The Si—O—Si, O_b—Si—O_b, O_t—Si—O_t, and Si—O—H angles are very similar in both calculations. Indeed, both calculations predict the same dipole moment for the closed conformation (0.35 D), but very different values (0.39 D and 1.55 D) for the straight one.

Linear Tetramer. As in the linear trimer, the lowest energy conformation found for the linear tetramer is almost cyclic, with hydrogen bonds linking the chain ends and forming a cyclic system, where each hydrogen is covalently bonded to an oxygen and coulombically attracted to another one. At the DF-BHL/DNP level of approximation, this curved conformation is 11.6 kcal mol^{-1} more stable than the straight conformation. The structure and charge distribution for both conformations are presented in Figure 4. The five hydrogen bonds in the curved conformation have an O- -H distance that is too short (1.51–1.68 Å) and an OH distance that is too large (1.01–1.05 Å), whereas the six hydrogen bonds in the straight conformation are much weaker (with O- -H distances between 1.92 Å and 2.11 Å).

Energies and Conformations of Silica-Based Clusters

J. Phys. Chem. A, Vol. 103, No. 17, 1999 **3259**

Si 4921-4964	SiO_b 1.63-1.65	$SiOSi$ 117.8-119.5
O_b 2782-2874	SiO_t 1.62-1.66	O_bSiO_b 111.9-113.0
O_t 2516-2996	OH 0.98-1.00	O_tSiO_t 108.3-114.6
H 1340-1398	O-H 1.92-2.11	$SiOH$ 108.2-114.0

Si 4611-4852
O_b 2151-2737
O_t 2313-2907
H 1038-1823

SiO_b 1.64-1.66
SiO_t 1.62-1.67
OH 0.98-1.03
O-H 1.51-1.68

$SiOSi$ 121.7-128.0
O_bSiO_b 108.5-109.7
O_tSiO_t 106.8-112.5
$SiOH$ 104.7-118.0

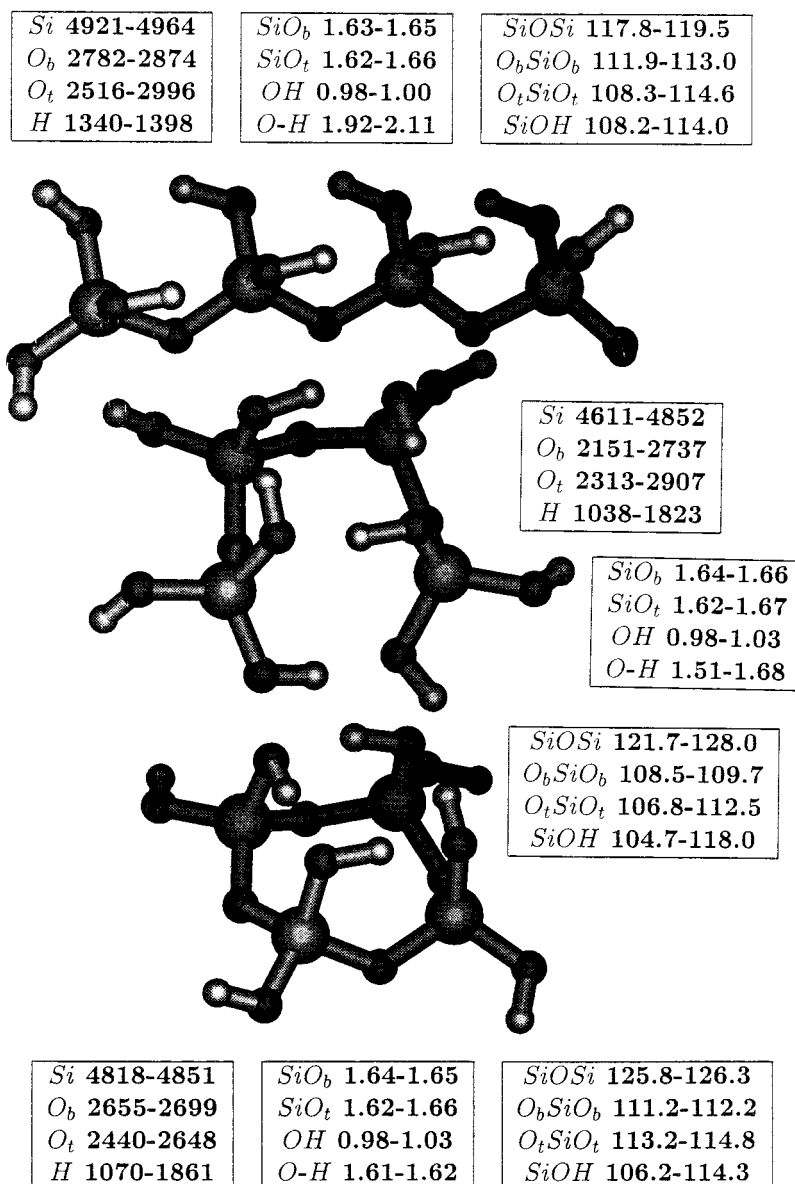| Si 4818-4851	SiO_b 1.64-1.65	$SiOSi$ 125.8-126.3
O_b 2655-2699	SiO_t 1.62-1.66	O_bSiO_b 111.2-112.2
O_t 2440-2648	OH 0.98-1.03	O_tSiO_t 113.2-114.8
H 1070-1861	O-H 1.61-1.62	$SiOH$ 106.2-114.3

Figure 4. Bond lengths (Å), bond angles (degrees), and Hirshfeld atomic charges (0. and minus sign in O charges are omitted) for $Si_4O_3(OH)_{10}$ conformations forming $Si_4O_4(OH)_8$, optimized at the DF-BHL/DNP level of approximation. Energy difference: (top) → (medium) $E = -11.6$ kcal mol^{-1}; (medium) → (below) $E = +12.4$ kcal mol^{-1}. Dipole moment: $\mu = 2.40$ D (above), $\mu = 2.75$ D (center), and $\mu = 0.65$ D (bottom).

Although the effect of improving the level of approximation is not clear, it seems reasonable to expect that the curved conformation would still be highly probable, in agreement with the experimental evidence, which shows that it is relatively easy to produce four-silicon rings. The easiest way to get a four-silicon ring is probably to close an open four-silicon linear chain, which should be particularly simple starting from this almost cyclic conformation.

The total condensation energy for the curved conformation (-38.2 kcal mol^{-1}) again appears to be too large when compared with the best calculations on the dimer. With application of the correction factor, previously estimated for each overestimated hydrogen bond, the corrected condensation energy for the most stable conformation is -21.7 kcal mol^{-1}. Even this value might still be too negative. We note that, because of its lower symmetry, this conformation has a higher electric dipole moment (2.75 D) than the corresponding straight conformation (2.40 D).

Linear Pentamer. The lowest energy conformation found for the linear pentamer is a relatively complex structure, which is almost cyclic, with four hydrogen bonds closing three secondary rings: two with 8 atoms and a third one with 10. At the DF-BHL/DNP level of approximation, this conformation is 11.4 kcal mol^{-1} more stable than the straight conformation. The structures and charge distributions for both conformations are presented in Figure 5.

The total condensation energy for the curved conformation is substantially negative (-43.6 kcal mol^{-1}). Even after correcting the energy, to account for the overestimation of the four hydrogen bonds, the condensation energy is 1.8 kcal mol^{-1} smaller than for the uncorrected straight conformation. It is reasonable, therefore, to expect that the almost cyclic conformation will remain a highly stable conformation at higher levels of approximation.

Despite its complexity, this conformation is remarkable because it allows the subsequent formation of several different clusters through a single intramolecular condensation reaction. If each of the four oxygen atoms bonded to hydrogens in different silicons (see Figure 5) reacts directly with these instead, in a nucleophilic attack, the five-silicon ring, the branched four-silicon ring, the branched three-silicon ring, and the double-

Si 4638-4678	SiO_b 1.63-1.65	$SiOSi$ 116.9-118.2
O_b 2538-2636	SiO_t 1.63-1.66	O_bSiO_b 110.0-112.8
O_t 2435-2887	OH 0.98-1.00	O_tSiO_t 108.4-115.1
H 1291-1851	$O-H$ 1.95-2.07	$SiOH$ 108.2-113.5

Si 4579-4890	SiO_b 1.62-1.66	$SiOSi$ 130.4-159.2
O_b 2559-2734	SiO_t 1.61-1.67	O_bSiO_b 105.8-116.1
O_t 2120-2930	OH 0.98-1.02	O_tSiO_t 106.6-112.4
H 0958-1916	$O-H$ 1.60-1.68	$SiOH$ 110.0-117.7
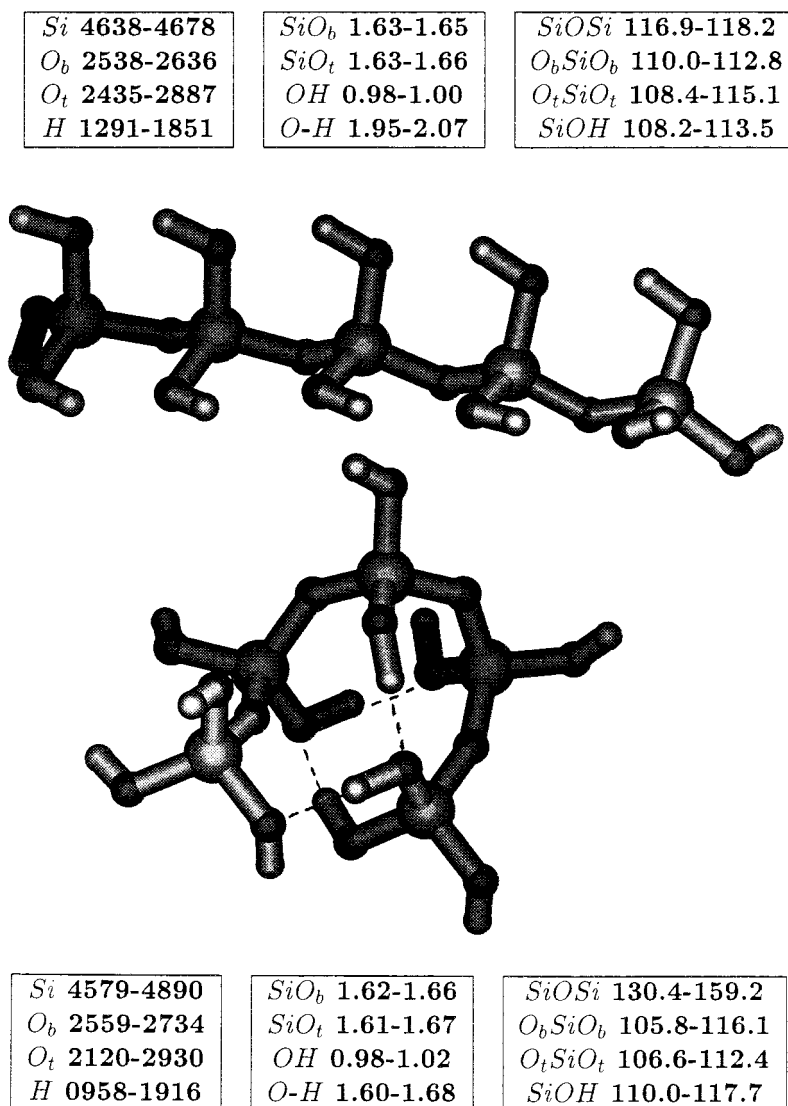
Figure 5. Bond lengths (Å), bond angles (degrees), and Hirshfeld atomic charges (0. and minus sign in O charges are omitted) for $Si_5O_4(OH)_{12}$ conformations, optimized at the DF-BHL/DNP level of approximation. Energy difference: (top) → (bottom) $E = -11.4$ kcal mol^{-1}. Dipole moment: $\mu = 2.70$ D (above) and $\mu = 2.23$ D (below).

branched three-silicon ring can be formed. The O- -H distance in the four hydrogen bonds is too short (1.60–68 Å) because of the overestimation of these bonds by the LDA approximation. We again note that the electric dipole moment is higher in the most stable conformation (3.23 D) than in the straight one (2.70 D) because of the highly asymmetric structure and charge distribution of the former.

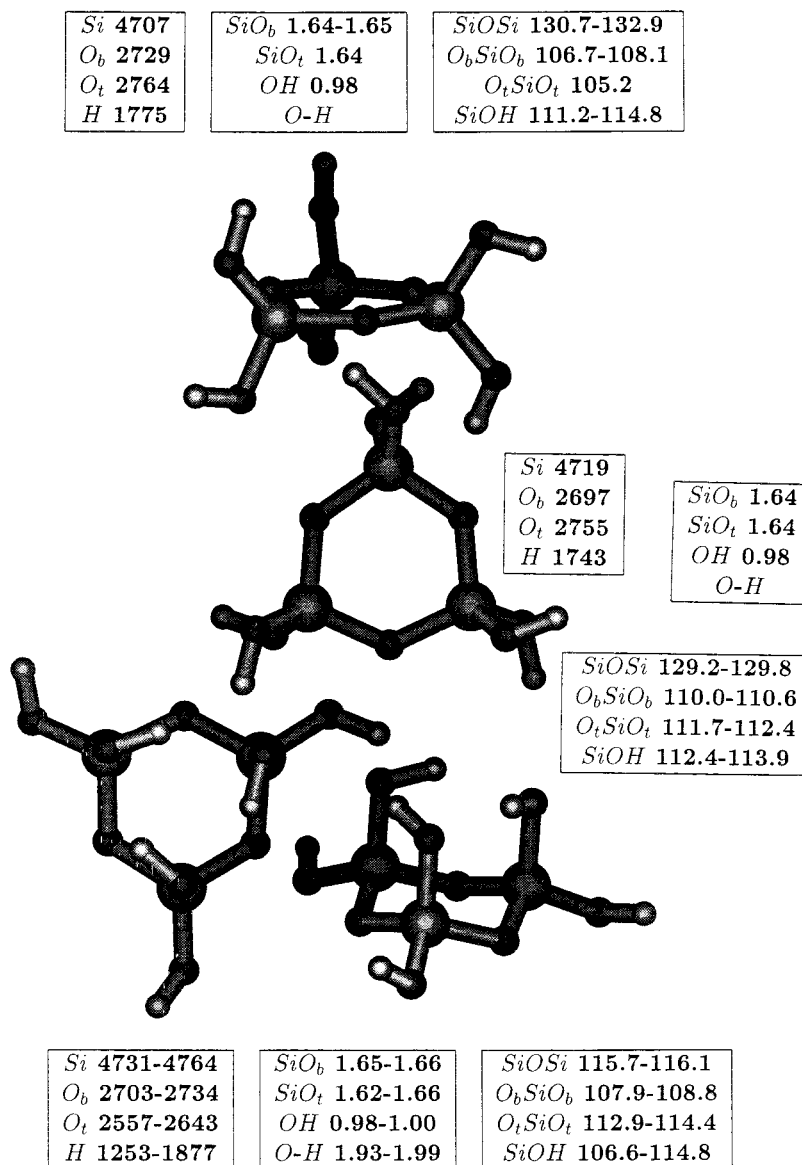*4.2.2. Structures.* In the linear trimer, the two Si–O bonds acting as hydrogen bond donors are weaker and longer (1.67–1.68 Å) than normal, whereas the other two, acting as hydrogen bond acceptors, are stronger and shorter (1.62 Å), because the oxygen charge can be redistributed more between the oxygen and silicon atoms. The primary bonds in both OH donor and OH acceptor groups are weaker, in the first case because of the charge transfer to the outer region, and in the second case, because the hydrogens are attracted to the outer oxygen. Hydroxyl groups acting simultaneously as donors and acceptors, where the oxygen and the hydrogen participate in different hydrogen bonds, show intermediate O–H and Si–O bond lengths.

In the linear tetramer, the four hydroxyl groups in equatorial positions present typical distances, for this level of approximation (Si–O = 1.63–1.64 Å and O–H = 0.98 Å). The Si–O bond length increases slightly for the four hydroxyl groups participating in the cyclic hydrogen bond system, 1.64–1.67 Å, whereas in the (isolated) fifth hydrogen bond, the Si–O bond length is 1.66 Å for the donor oxygen and 1.62 Å for the oxygen bonded to the acceptor hydrogen.

In the linear pentamer, the Si–O and O–H bond lengths in unconstrained outer hydroxyl groups (1.63–1.64 Å and 0.98–0.99 Å) are similar to the values calculated for other clusters. As in the linear trimer and tetramer, the two OH groups that act only as donors have larger OH and SiO distances (0.99 Å and ≈1.66 Å), whereas the two OH acceptor groups have larger OH distances (1.02 Å) but smaller Si–O lengths, 1.61–1.63 Å. The pentamer straight conformation, with weaker hydrogen bonds (O–H equal to 1.94–2.13 Å), shows intermediate values for the Si–O and O–H bond lengths and relatively small Si–O–H angles (<113.5°) because of the directionality of the hydrogen bonds.

The Si–O–Si angles are significantly larger in the linear trimer (≈141°) than in the dimer because of its almost cyclic arrangement. (In the trimer straight conformation, these angles are 120.3°.) In the linear tetramer, the middle Si–O–Si is about 6° smaller than the other two, although the O_b–Si–O_b angle remains almost constant. The Si–O–H angles vary between

| Si 4707 |
| O_b 2729 |
| O_t 2764 |
| H 1775 |

| SiO_b 1.64-1.65 |
| SiO_t 1.64 |
| OH 0.98 |
| O-H |

| $SiOSi$ 130.7-132.9 |
| O_bSiO_b 106.7-108.1 |
| O_tSiO_t 105.2 |
| $SiOH$ 111.2-114.8 |

| Si 4719 |
| O_b 2697 |
| O_t 2755 |
| H 1743 |

| SiO_b 1.64 |
| SiO_t 1.64 |
| OH 0.98 |
| O-H |

| $SiOSi$ 129.2-129.8 |
| O_bSiO_b 110.0-110.6 |
| O_tSiO_t 111.7-112.4 |
| $SiOH$ 112.4-113.9 |

| Si 4731-4764 |
| O_b 2703-2734 |
| O_t 2557-2643 |
| H 1253-1877 |

| SiO_b 1.65-1.66 |
| SiO_t 1.62-1.66 |
| OH 0.98-1.00 |
| O-H 1.93-1.99 |

| $SiOSi$ 115.7-116.1 |
| O_bSiO_b 107.9-108.8 |
| O_tSiO_t 112.9-114.4 |
| $SiOH$ 106.6-114.8 |

Figure 6. Bond lengths (Å), bond angles (degrees), and Hirshfeld atomic charges (0. and minus sign in O charges are omitted) for $Si_3O_3(OH)_6$ conformations, optimized at the DF-BHL/DNP level of approximation. Energy difference: (top) → (medium) $E = -0.8$ kcal mol^{-1}; (medium) → (below) $E = -5.3$ kcal mol^{-1}. Dipole moment: $\mu = 1.53$ D (above), $\mu = 0.35$ D (center), and $\mu = 1.68$ D (bottom).

104.7° (in the constrained system of four hydrogen bonds) and 118.0° (in the equatorial free Si—O—H groups), almost matching Sauer's reference value for the monomer.[17]
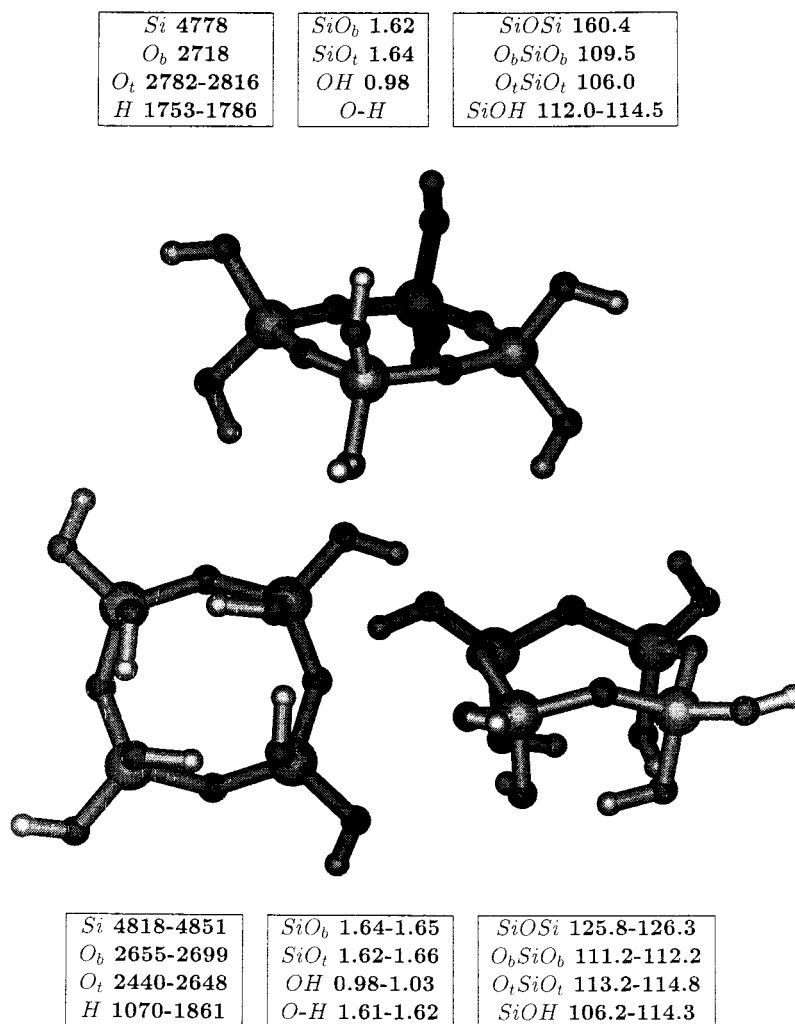
In the linear pentamer, the Si—O—H angle is very similar for terminal and constrained OH groups (111.5—115.0° and 110.0—117.7°), respectively. We find significant changes for the O_b—Si—O_b angle along the chain (105.8—116.1°), although the Si—O—Si angles are clearly much softer, varying over a large range (between 130.4 and 159.2°), which reflects the asymmetry of this conformation. Despite the hydrogen bonds, the O_t—Si—O_t angles are very similar in all these clusters (106.5—112.5°).

4.3. Ring Structures: Trimer and Tetramer Ring, Octamer Cage. *4.3.1. Energy and Conformations. Trimer Ring.* Figure 6 shows the structure and charge distribution for the three most important conformations found in this work for the cyclic trimer. At the DF-BHL/DN level, the first conformation is +5.0 kcal mol^{-1} more stable than the second, but at the DF-BHL/DNP level, the energy of the second conformation is 0.8 kcal mol^{-1} lower. Thus, the order in energy of these conformations changed, simply by adding polarization functions to the basis

set. This was the only case throughout this work where such an effect was observed, and indeed, the influence of the calculation method on the results is expected to decrease significantly when the level of accuracy increases.

In fact, none of these planar ring conformations represents the global energy minimum for this cluster. The third conformation represented in Figure 6 is 5.3 kcal mol^{-1} more stable than the second (at the DF-BHL/DNP level) and is the lowest energy conformation that we found for the ring trimer. It has a *chair* conformation (as in 6-carbon rings), where three hydroxyl groups occupy equatorial positions, and the other three are disposed in axial positions, forming a strong system of three hydrogen bonds. At this level of approximation, the total energy of condensation is still exothermic (−1.6 kcal mol^{-1}), despite the strain associated with this ring. At the DF-BLYP/DNP level of approximation, the total condensation energy is already positive but still small (+5.5 kcal mol^{-1}), so this cluster should be present in silica solutions, as experimental evidence shows, despite its internal strain.

The relative orientations of the equatorial and axial OH groups can be the same (clockwise—clockwise) or opposite (clockwise-

Si 4778	SiO_b 1.62	$SiOSi$ 160.4
O_b 2718	SiO_t 1.64	O_bSiO_b 109.5
O_t 2782-2816	OH 0.98	O_tSiO_t 106.0
H 1753-1786	O-H	$SiOH$ 112.0-114.5

Si 4818-4851	SiO_b 1.64-1.65	$SiOSi$ 125.8-126.3
O_b 2655-2699	SiO_t 1.62-1.66	O_bSiO_b 111.2-112.2
O_t 2440-2648	OH 0.98-1.03	O_tSiO_t 113.2-114.8
H 1070-1861	O-H 1.61-1.62	$SiOH$ 106.2-114.3

Figure 7. Bond lengths (Å), bond angles (degrees), and Hirshfeld atomic charges (0. and minus sign in O charges are omitted) for $Si_4O_4(OH)_8$ conformations, optimized at the DF-BHL/DNP level of approximation. Energy difference: (top) $\rightarrow$ (bottom) $E = -31.9$ kcal mol^{-1}. Dipole moment: $\mu = 0.01$ D (above), $\mu = 0.65$ D (below).

counterclockwise). The question of their relative stabilities was investigated at the DF-BLYP/DNP level of approximation; the conformation with the same orientation for both axial and equatorial OH groups was found to be slightly more stable ($+1.4$ kcal mol^{-1}). This energy difference is very small, because the equatorial hydrogens are isolated and may change for a larger basis set.

For both levels of approximation, the axial hydrogens have smaller charges than the equatorial ones (because of the axial hydrogen bonds), but the oxygen charges are very similar. Despite its higher symmetry, this cluster seems to have a much larger charge separation than the open trimer, apparently because of the different orientations of the two sets of hydroxyl groups. In fact, the dipole moment for the DF-BLYP/DNP calculation is probably too high and will change significantly when better basis sets are used.

Tetramer Ring. The lowest energy conformation found for the four-silicon ring is a crown conformation (the most stable conformation in 8-carbon rings[54]), which decreases the ring strain and allows the formation of a strong cyclic system of four hydrogen bonds, decreasing considerably the energy of the cluster. At the DF-BHL/DNP level of approximation, this conformation is 31.9 kcal mol^{-1} more stable than the planar one, which is highly symmetric but with relatively weak hydrogen-bond interactions. This difference in energy is the
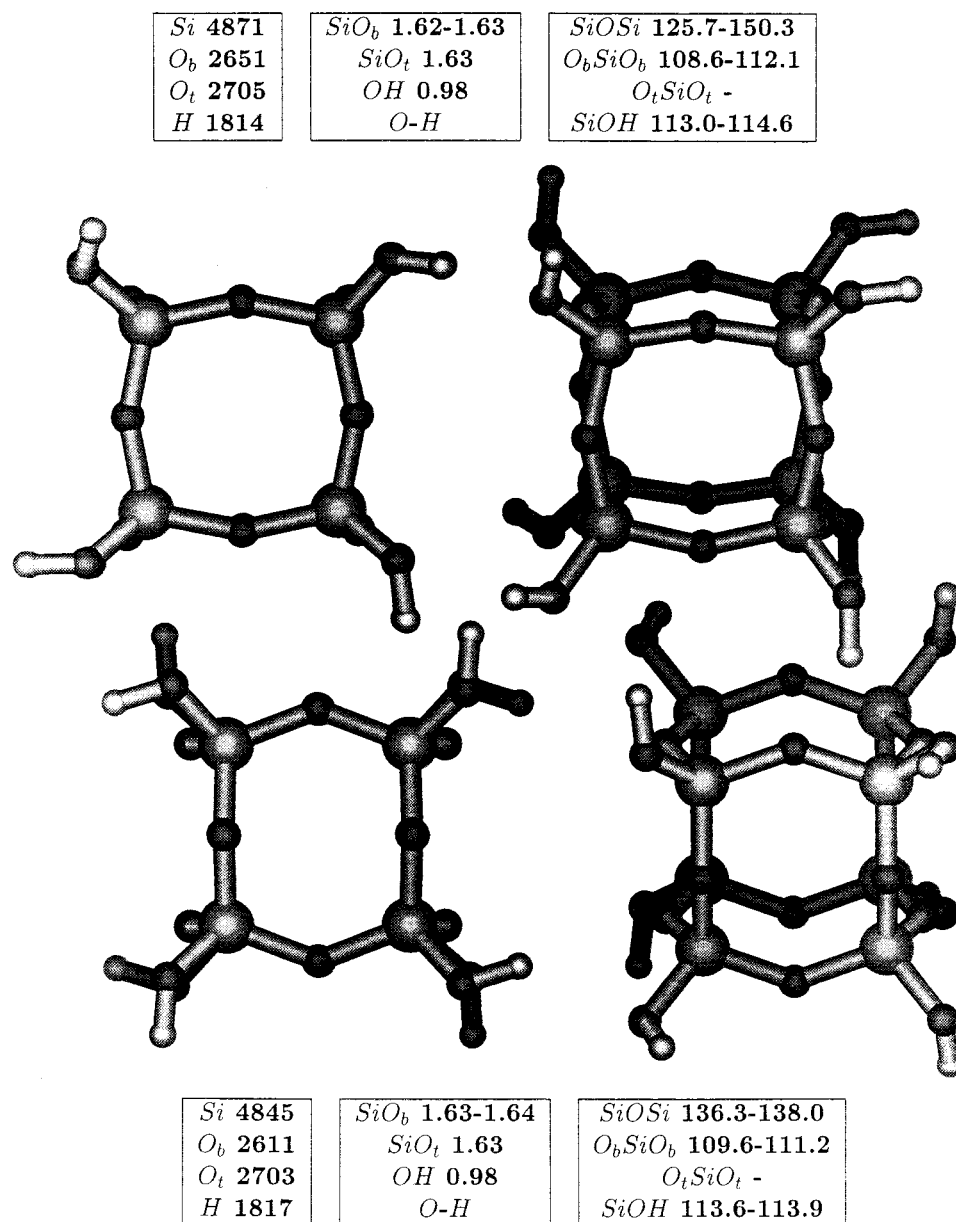
largest found throughout all this work between two conformations of the same cluster. The structure and charge of both conformations are shown in Figure 7.

Although the ring strain should be considerably smaller in this cluster than in the more constrained trimer ring, the total condensation energy for the crown conformation (-25.7 kcal mol^{-1}) appears to be too negative, when compared with the nonlocal density results obtained for the two- and three-silicon clusters. Furthermore, it is only 5 kcal mol^{-1} higher than the corresponding value for the branched tetramer. This is essentially due to the overestimation by the LDA method of the four hydrogen bonds, whose bond length is too short (≈ 1.62 Å). Correcting the energy, following the results for the dimer, the condensation energy becomes -12.5 kcal mol^{-1}, which is more acceptable.

Despite the very different atomic arrangements on both sides of the ring, the cluster with a crown conformation has a relatively small electric dipole (0.65 D), much smaller than in the other four-silicon clusters (or even in the three-silicon ring, with a similar hydrogen bond system). The electric dipole moment of the planar conformation is zero, as is required by its symmetry.

Octamer Cage. The structure and charge distributions for the most important conformations of the octamer cage (particularly important in zeolite catalysts) are shown in Figure 8. These

Si **4871**	*SiO$_b$* **1.62-1.63**	*SiOSi* **125.7-150.3**
O$_b$ **2651**	*SiO$_t$* **1.63**	*O$_b$SiO$_b$* **108.6-112.1**
O$_t$ **2705**	*OH* **0.98**	*O$_t$SiO$_t$* **-**
H **1814**	*O-H*	*SiOH* **113.0-114.6**

Si **4845**	*SiO$_b$* **1.63-1.64**	*SiOSi* **136.3-138.0**
O$_b$ **2611**	*SiO$_t$* **1.63**	*O$_b$SiO$_b$* **109.6-111.2**
O$_t$ **2703**	*OH* **0.98**	*O$_t$SiO$_t$* **-**
H **1817**	*O-H*	*SiOH* **113.6-113.9**

Figure 8. Bond lengths (Å), bond angles (degrees), and Hirshfeld atomic charges (0. and minus sign in O charges are omitted) for Si$_8$O$_{12}$(OH)$_8$ conformations, optimized at the DF-BHL/DNP level of approximation. Energy difference: (top) → (bottom) $E = -1.6$ kcal mol^{-1}.

conformations differ only in the atomic arrangement of the four-silicon rings forming the six faces of the cubic cage. In one conformation, the rings have a crown arrangement, as in the tetramer ring, whereas in the other they have a nonplanar hexagonal arrangement, in which each oxygen is in the plane of one face of the cube and out of the plane of the face adjacent. Each ring in the cage defines a window, which is almost circular in the crown arrangement (of dimensions 3.8 Å × 3.8 Å), and rectangular in the hexagonal arrangement (of dimensions 4.2 Å × 3.1 Å).

There are no hydrogen bonds in this cluster, because the hydroxyl groups are too far apart. Consequently, the energy and structure obtained with LDA should be particularly accurate and the energy difference between the two conformations should be essentially due to the framework of the two cages. At the DF-BHL/DNP level of approximation, the "six-hexagon" conformation is +1.6 kcal mol^{-1} more stable than the "six-crown" conformation. Replacing the hydroxyl groups by hydrogen atoms, the difference in energy between the two conformations decreases to only 0.5 kcal mol^{-1}.

The condensation energy for Si$_8$O$_{12}$(OH)$_8$, although positive (+4.1 kcal mol^{-1}), seems reasonable for this relatively strained cluster. ^{29}Si NMR experimental evidence show that this species is relatively stable in solution, at least for high pH values, although it has been found in only small concentrations.[9,13,14] The corresponding HF result of Hill and Sauer[20] for the crown conformation (−4.9 kcal per mole of Si−O bonds) suggests a greater stability than might be expected for a constrained cage, which cannot form intramolecular hydrogen bonds. As expected for such a highly symmetric conformation, the electric dipole moment is zero.

4.3.2. Structures. In the ring trimer conformation with the higher energy, the O$_t$−Si−O$_t$ angle is smaller because of the interaction between adjacent hydroxyl groups. The Si−O−Si angle is much larger in the two planar rings than in the chair conformation (≈116.0°). In this conformation, the Si−O−Si, O$_b$−Si−O$_b$, and O$_t$−Si−O$_t$ angles change very little, because of the symmetry constraints imposed by the ring and the directionality of the hydrogen bonds. The Si−O−H angle assumes two distinct values, one for the equatorial hydroxyl
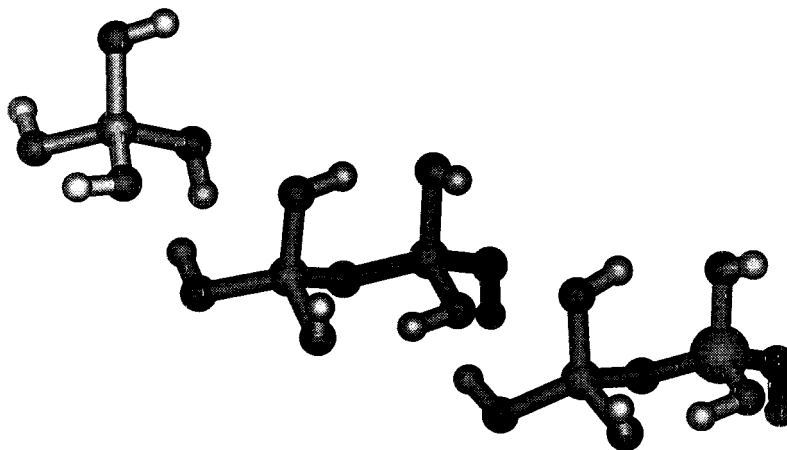
Figure 9. $Al(OH)_4^-$, $Al_2O(OH)_6^{2-}$, and $AlSiO(OH)_6^-$ clusters after ab initio DFT-BHL/DNP energy minimization.

groups ($\approx 114.5°$, as in previous clusters), and another, which is much smaller ($\approx 106.8°$), for the axial hydroxyl groups, that are constrained to assume values closer to 90°, by the directionality of the hydrogen bonds.

As we noted earlier, the atoms involved in hydrogen bonds tend to form weaker primary bonds with longer bond lengths. In the ring trimer, where each axial oxygen simultaneously donates charge to a hydrogen and is bonded to an acceptor hydrogen, the $Si-O_t$ and $O-H$ bond lengths are $1.66-1.67$ Å and 1.00 Å, whereas these values decrease to 1.62 Å and 0.98 Å, respectively, in the equatorial hydroxyl groups. The $Si-O_b$ bond length in the ring is $0.02-0.03$ Å larger than the corresponding bond length in the open trimer because of the strain present in such a small ring. At the DF-BHL/DNP level of approximation, the O- -H distances ($1.93-1.99$ Å) are much larger than in the open trimer, owing to the balance between the electrostatic forces that tend to move the hydroxyl groups closer and the covalent forces that tend to move them further apart (to decrease the ring strain). At the DF-BLYP/DNP level, where hydrogen bonds are not overestimated, the O- -H distances are already much longer ($2.69-3.01$ Å) than in the linear trimer. The $Si-O-Si$ angle in the trimer ring is larger in the DF-BLYP/DNP calculation ($121.3-122.4°$) than in the DF-BHL/DNP ($115.7-116.1°$).

In the tetramer ring, the $Si-O$ bond length is calculated as 1.62 Å in the equatorial groups, as $1.64-1.65$ Å in the ring, and as 1.66 Å in the terminal groups forming hydrogen bonds. The $O-H$ bond length is calculated as 0.98 Å in the four equatorial hydroxyl groups (a normal value for this level of approximation) but is too large in the four hydrogen bonds (1.03 Å). In the planar conformation, where hydrogen bonds are much weaker, the $Si-O$ bond length follows exactly the opposite trend, being smaller in the ring (1.62 Å) than in the terminal groups (1.64 Å).

In the four-silicon ring, the $Si-O-Si$ angles ($125.8-126.3°$) are larger than in the three-silicon ring ($115.7 - 116.1°$); the O_b-Si-O_b angles ($111.2-112.2°$) are closer to the tetrahedral value than the O_t-Si-O_t angles ($113.2-114.8°$), although these should be less constrained. The $Si-O-H$ angle assumes two different sets of values, one in the equatorial hydroxyl groups ($113.3-114.3°$) and another that is much smaller in the axial hydroxyl groups ($\approx 106.4°$), because of the effects of the hydrogen bonds. The $Si-O-Si$ angle is much larger ($160.4°$) in the planar conformation, reflecting the different atomic arrangements of the two rings.

In the cubic cage, the $Si-O-Si$ angles are almost constant in the more stable conformation (and larger than in acyclic

systems), but they change considerably in the six-crown conformation. This large range of variation and the small energy difference between the two conformations shows once again that the $Si-O-Si$ angle is extremely soft. The bond lengths and O_b-Si-O_b and $Si-O-H$ bond angles are essentially constant and equal in both conformations.

Studying $Si_8O_{12}H_8$ has the additional advantage of permitting us to compare the calculated values with the experimental data available for this cluster. As determined by Larsson (see ref 34), the $Si-H$ and $Si-O$ bond lengths and the $O-Si-H$, $O-Si-O$, and $Si-O-Si$ bond angles are, respectively, 1.475 Å and 1.659 Å, and $112.2°$, $106.6°$, and $153.9°$. The $Si-O$ bond length and $Si-O-Si$ bond angle are relatively large.

4.4. $Al(OH)_4^-$, $Al_2O(OH)_6^{2-}$, and $AlSiO(OH)_6^-$. In addition to silica clusters, we have also examined the smallest alumina-based clusters, $Al(OH)_4^-$, $Al_2O(OH)_6^{2-}$, and $AlSiO(OH)_6^-$, (shown in Figure 9). The main data on structure and charge distribution obtained for these clusters, at the DF-BHL/DNP level of approximation, are presented in Table 4.

The properties of these clusters are closely related to their electrical charge. The electric dipole moment becomes very high for the nonsymmetrical species, as the additional charge results in a much more diffuse electron density distribution.

As in the silica dimer, both $Al_2O(OH)_6^{2-}$ and $AlSiO(OH)_6^-$ have two hydrogen bonds, which we expect to be overestimated, at this level of approximation. Because the charge separation is large, these hydrogen bonds should be particularly strong, which is confirmed by the smallest O- -H distance in both clusters, calculated as 1.55 Å and 1.89 Å. The charges in the oxygen atoms bonded to aluminum are significantly larger than in the oxygens bonded to silicon, which explains why, in the aluminosilicate cluster, the hydrogen bond formed by the aluminum-bonded oxygen is much stronger (1.55 Å) than those formed by silicon-bonded oxygen (2.21 Å). This result is confirmed by the corresponding OH distances in the acceptor hydroxyl groups, which are 1.05 Å and 0.99 Å, respectively.

As in the silica clusters, the $Al-O$ and $Si-O$ bonds become much weaker when the oxygen atoms form hydrogen bonds, because of the charge transfer to the outer hydrogens, resulting in longer bond lengths of 1.81 Å and 1.69 Å, respectively. The $Al-O-H$ and $Si-O-H$ angles are smaller in these than in the related silica clusters, apparently because of the charge distribution. The $Al-O-Al$ angle is smaller than for $Al-O-Si$, which in turn is smaller than for $Si-O-Si$, for the same DF-BHL/DNP level of approximation.

At this level of theory, the condensation energy to form $Al_2O(OH)_6^{2-}$ and $AlSiO(OH)_6^-$, from $Al(OH)_4^-$ and $Si(OH)_4$,

Energies and Conformations of Silica-Based Clusters

J. Phys. Chem. A, Vol. 103, No. 17, 1999 **3265**

is calculated as +61.7 kcal mol^{-1} and −27.2 kcal mol^{-1}, respectively. The first reaction is highly endothermic because two species with charge −1 are transformed into a single species with charge −2, which is therefore much less stable. The second reaction is highly exothermic because both reactants and products have a charge of 1, and this excess can be spread across a wider region in the larger product species, which therefore becomes more stable. These results show that, in gas-phase studies of charged species, the energies are essentially controlled by the charge distribution and depend very little on structural factors. This conclusion is confirmed by the results that we obtained for the mechanism of the condensation reaction, which are presented elsewhere.[55]

5. Conclusions

The strong hydrogen bonds formed by hydroxyl groups and the flexibility of the Si−O−Si angle are the most important features of the chemistry of silica clusters in vacuo, leading to the formation of different conformations with significant differences in energy, structure, and charge distribution. However, local properties such as bond lengths and partial charges change very little, unless strong hydrogen bonds are involved directly. When this is the case, the results (especially the energies) obtained with LDA need to be corrected.

Conformations with significantly different energies are found even in small clusters such as the dimer. In the monomer and cubic cage, where there are no hydrogen bonds, the differences in energy are very small. Different arrangements in the cubic cage have almost the same energy because they are formed by Si−O−Si linkages. The chair and crown arranagements in the trimer and tetramer rings are very stable, because they allow the formation of strong systems of hydrogen bonds. In some cases, when the energy barrier is very small, the order of stability of two conformations can be inverted on changing only the basis set.

In the gas phase, the straight conformations of the trimer, tetramer, and pentamer linear clusters are less stable than the curved ones, where the two ends of the chain interact directly, forming almost cyclic structures. These, in turn, can react directly by an intramolecular condensation to form the corresponding rings. These results suggest that there is an intramolecular mechanism for the ring formation in silicates. However, the trend to adopt ring-like conformations is likely to be reduced in the liquid phase, and further calculations are necessary to clarify this point.

The energy of the condensation reaction between neutral species is calculated to be small (<3 kcal/mol), although it strongly depends on the charges involved, as shown by the charged alumina species. The work that we have reported will help in developing a systematic analysis of the smallest silica species occurring in silica-based processes, thus contributing to a better understanding of these systems, so important in scientific and technological applications.

Appendix A: Accuracy of Computational Procedures

To assess the accuracy of the procedures used in this study we report results on the widely studied water molecule and dimer.

TABLE 7: Bond Length (Å), Bond Angle (deg), and Electric Dipole (Debye) for an Isolated H$_2$O Molecule after Local DF-BHL, Nonlocal DF-BLYP, and HF-MP2 Optimizations Using Numerical (DNP, TNP) and Gaussian (6-31G, 6-311G**) Basis Sets**

method	H$_2$O		
	OH length	H−O−H angle	dipole
BHL/DNP	0.98	103.9	1.86
TNP	0.97	104.8	1.87
BLYP/DNP	0.99	103.8	1.80
TNP	0.97	104.9	1.81
MP2/6-31G**	0.96	103.8	2.11
6-311G**	0.96	102.4	2.10
exp[57,63]	0.9584	104.45	1.85

TABLE 8: Hydrogen Bond Energy (kcal mol^{-1}) Bond Lengths (Å), Bond Angles (deg), and Electric Dipole (Debye) for an Isolated H$_2$O- -H$_2$O Water Dimer

method	H$_2$O- -H$_2$O						
	hyd. E	O−O	O−H	O- -H	OH- -O	H- -O⟨OH⟩^{a}	dipole
BHL/DNP	−11.3	2.71	1.00	1.71	176.9	106.0	2.66
TNP	−9.0	2.71	0.99	1.72	176.6	106.2	2.65
BLYP/DNP	−6.4	3.01	0.99	2.02	175.9	116.9	2.59
TNP	−4.3	2.98	0.98	2.00	172.7	119.1	2.44
MP2/6-31G**	−7.1	2.92	0.96	1.96	169.9	107.3	2.28
gas	−5.3	2.98				180	120
ice I_h (100 K)	−6.0		1.01	1.74		180	120

^{a} ⟨H⟩ means the bisector line between the two hydrogens in the donor molecule. Experimental values are from refs 58, 60, and 61.

H$_2$O. Table 7 shows the results for the structure and charge distribution of a single molecule of water for several levels of approximation. At the DF-BHL/DNP level (with local density and a double basis set with polarization functions), the calculated O−H bond length (0.98 Å), H−O−H bond angle (103.9°), and electric dipole moment (1.86 D) are already very close to the experimental values, 0.9548 Å, 104.45°, and 1.85 D, respectively.[56,57] Use of a triple basis set (at the DF-BHL/TNP level) increases only slightly the accuracy of the calculated O−H bond length (which becomes 0.97 Å) and increases the H−O−H angle to 104.8°.

In the nonlocal density calculation, with a double basis set (DF-BLYP/DNP), the accuracy of the O−H bond length (0.99 Å) decreases slightly when compared with the local density determinations. The best calculation presented in this work for water, a nonlocal density calculation with a triple basis set (DF-BLYP/TNP), leads to very precise results for the O−H bond length, the H−O−H bond angle, and the electric dipole moment, only 0.01 Å, 0.4°, and 0.04 D from the experimental data, respectively. The HF method, at the MP2 level, with a 6-31G** double-ζ plus polarization basis set, leads to a O−H bond length that matches the experimental value (0.96 Å), but the dipole moment is too high (2.11 D).

H$_2$O- -H$_2$O. The description of the structure and energy of a hydrogen bond is a difficult test for any ab initio method. The results presented in Table 8 for an isolated water dimer show important differences between the various ab initio methods tested. The H-bond energy predicted by the LDA (−11.3 kcal mol^{-1}) is much higher than the experimental value for the water dimer of −5.0 kcal mol^{-1}.[58,59] Furthermore, the calculated H-bond length (1.71 Å) is too short when compared with the value predicted from experiment for gas-phase species of 1.98−2.00 Å.[60] However, similar O−H bond lengths of 1.74 Å and 1.01 Å, respectively, were found in ice I_h at 100 K.[61] An LDA calculation, with a triple basis set (DF-BHL/TNP), leads to a small improvement in the hydrogen bond energy (−9.0 kcal mol^{-1}), but the O- -H bond length remains almost unaltered.

3266 *J. Phys. Chem. A, Vol. 103, No. 17, 1999*

Pereira et al.

TABLE 9: Bond Length (Å) and Electric Dipole (Debye) for an Isolated OH⁻ Ion

	OH^-		
method	BHL/DNP	BLYP/DNP	MP2/6-31G**
OH length	0.99	0.99	0.97
dipole	0.16	0.19	0.99

TABLE 10: Bond Length (Å), Bond Angle (deg), and Electric Dipole (Debye) for an Isolated H_3O^+ Ion

	H_3O^+			
method	BHL/DNP	BLYP/DNP	MP2/6-31G**	exp[56]
OH length	1.01	1.01	0.98	0.95
H−O−H angle	108.3	108.3	112.6	109
dipole	2.25	2.22	2.26	

Much better agreement with the experiment is found when nonlocal DF with a double basis set is used (DF-BLYP/DNP). The hydrogen bond energy decreases to -6.4 kcal mol^{-1}, which is still $1-2$ kcal mol^{-1} higher than the experimental value, and the O- -H bond length (2.02 Å) becomes only $0.02-0.04$ Å larger than the value predicted from experiment. A further improvement is achieved when a triple basis set is used (DF-BLYP/TNP): the hydrogen bond energy decreases to -4.3 kcal mol^{-1}, close to the values predicted by the best HF calculations (about -4.5 kcal mol^{-1} [59]), and the distance between the two oxygen atoms (2.98 Å) matches exactly the experimental value.[60]

In DF-BHL/DNP and HF-MP2/6-31G** calculations, the H- -O-⟨H⟩ angle (where ⟨H⟩ indicates the bisector line between the hydrogens in the donor molecule) is about 15° smaller than the experimental value of 120°.[60] However, in both nonlocal DF calculations, the agreement with experiment is excellent, particularly with a triple basis set (DF-BLYP/TNP). For all calculations, the O−H−O angle is relatively close to the value predicted by experiment, 180°,[60] although it decreases when the level of approximation increases.

The HF calculation predicts a good value for the O- -H hydrogen bond length (1.96 Å), but the corresponding O−H bond length is too short (0.96 Å) and consequently the O- -O distance is 0.06 Å shorter than the experimental value. As can be seen for ice I_h,[61] or by comparing the DF-BLYP/TNP calculations in the water dimer with those for a water molecule, hydrogen bonding tends to increase the primary O−H bond length. The HF value for the hydrogen bond energy is relatively poor (-7.1 kcal mol^{-1}) at this level of approximation, when compared with the nonlocal DF results, with a triple or even double basis set.

The water dimer has a large electric dipole moment, which according to the calculations presented here is probably between 2.28 D and 2.44 D for the best HF and DF results.

H_3O^+, OH⁻. The results presented in Tables 9 and 10 for the simplest ions, OH⁻ and H_3O^+, show almost no differences between the local and nonlocal DF values. However, the HF/MP2 results are significantly different. In particular, DF and HF predict very different values for the OH⁻ electric dipole moment (0.19 D and 0.99 D, respectively), which is surprising, considering the simplicity of this ion. However, the H_3O^+ dipole moment is almost the same in all calculations ($\approx$2.25 D) and is probably a reliable value.

The difference between DF and HF results for O−H bond lengths ($\approx$0.02$-$0.03 Å) is essentially the same as in water. The published ideal gas value for the O−H bond length in H_3O^+, 0.95 Å,[56] is probably too short, because this bond should be weaker and consequently longer than in H_2O, where the

TABLE 11: Water Auto-ionization Energy (kcal/mol), after Local DF-BHL, Nonlocal DF-BLYP, and HF-MP2 Optimizations, using Numerical (DNP) and Gaussian (6-31G) Basis Sets**

method	auto-ionization energy
BHL/DNP	221.0
BLYP	222.7
MP2/6-31G**	255.7
exp[56] (ΔH_f^0)	221.8

experimental bond length is 0.9584 Å.[56] An increase of about 0.02 Å in the O−H bond length is actually predicted in all three calculations for this ion, and the real value should be very close to 0.98 Å, as calculated at the HF-MP2/6-31G** level.

The enthalpy of water auto-ionization ($2H_2O + \Delta H \rightarrow H_3O^+ + OH^-$), calculated from the heats of formation of H_2O, H_3O^+, and OH⁻ at 0 K,[56] is shown in Table 11 and compared with the DF and HF results obtained from the total energy of the species involved. The agreement is excellent for both local and nonlocal DFT calculations but is relatively poor for the MP2 method, which is 33.9 kcal mol^{-1} higher than expected.

Appendix B: Basis Sets

The five hydrogen radial functions in Dmol were obtained from three atomic DFT calculations:[39] the first for the normal atom of hydrogen, to determine the occupied 1s orbital; the second with a nuclear charge of 1.3, to give additional 1s and 2p functions, slightly more contracted; and the third with a nuclear charge of 4.0, to obtain a further set of 1s and 2p functions, thereby generating an even better description, particularly near the nucleus.

The ten radial functions for oxygen were obtained after four atomic DFT calculations: the first for the normal oxygen atom, to give the occupied 1s, 2s and 2p functions; the second for the O^{2+} cation, where two electrons were removed from the higher 2p energy levels, to obtain a second set of 2s and 2p functions, closer to the nucleus; the third for a nuclear charge of +5.0 and a single electron, to give 3d, 2p, and 1s highly contracted functions; and the fourth for a nuclear charge of +7.0, again with a single electron, to obtain a additional set of 3d and 2p, giving the best possible description near the nucleus.

Thirteen radial functions were generated for silicon by undertaking three atomic DF calculations: first for the normal silicon atom, to give the occupied 1s+2s+2p+3s+3p five atomic orbitals; second for the ionic Si^{2+}, removing two α electrons from the highest energy 3p orbital and adding a 3d orbital, without changing its occupation to determine additional 3s+3p+3d functions;[39] and third for the ionic excited state formed when two α electrons leave 2s and 2p levels and one is transferred to a formerly empty 3d orbital, forming a Si^+ ion, to obtain another five basis functions, 2s+2p+3s+3p+3d.

References and Notes

(1) Iler, R. K. *The Chemistry of Silica*; John Wiley & Sons: New York, 1979.

(2) Keefer, K. D. In *Better Ceramics Through Chemistry*; Brinker, C. J.; Clark, D. E.; Ulrich, D. R., Eds.; Materials Research Society, Elsevier Science Publishing Co., Inc.: New York, 1984, p 15.

(3) Orcel, G.; Hench, L. *J. Non-Cryst. Solids* **1986**, *79*, 177.

(4) Balfe, C. A.; Martinez, S. L. In *Better Ceramics Through Chemistry II*; Brinker, C. J.; Clark, D. E.; Ulrich, D. R., Eds.; Materials Research Society, Vol. 73; Elsevier Science Publishing Co., Inc.: 1986; p 27.

(5) Pouxviel, J. C.; Boilot, J. P. *J. Non-Cryst. Solids* **1987**, *94*, 374.

(6) Tallant, D. R.; Bunker, B. C.; Brinker, C. J.; Balfe, C. A. In *Better Ceramics Through Chemistry II*; Brinker, C. J.; Clark, D. E.; Ulrich, D. R., Eds.; Materials Research Society, Vol. 73; Elsevier Science Publishing Co., Inc.: New York, 1986; p 261.

(7) Kinrade, S. D.; Swaddle, T. W. *Inorg. Chem.* **1988**, *27*, 4259.

Energies and Conformations of Silica-Based Clusters

J. Phys. Chem. A, Vol. 103, No. 17, 1999 **3267**

(8) Jonas, In *Ultrastructure Processing of Advanced Materials*; Uhlmann, D. R.; Ulrich, D. R., Eds.; John Wiley & Sons, Inc.: New York, 1992; Chapter 2, p 13.

(9) Klemperer, W. G.; Mainz, V. V.; Millar, D. M. In *Better Ceramics Through Chemistry II*; Brinker, C. J.; Clark, D. E.; Ulrich, D. R., Eds.; Materials Research Society, Vol. 73; Elsevier Science Publishing Co., Inc.: New York, 1986; p 3.

(10) Klemperer, W. G.; Mainz, V. V.; Millar, D. M. In *Better Ceramics Through Chemistry II*; Brinker, C. J.; Clark, D. E.; Ulrich, D. R., Eds.; Materials Research Society, Vol. 73; Elsevier Science Publishing Co., Inc.: New York, 1986; p 15.

(11) Klemperer, W. G.; Ramamurthi, S. D. In *Better Ceramics Through Chemistry III*; Brinker, C. J.; Clark, D. E.; Ulrich, D. R., Eds.; Materials Research Society, Vol. 121; Elsevier Science Publishing Co., Inc.: New York, 1988; p 1.

(12) Klemperer, W. G.; Mainz, V. V.; Ramamurthi, S. D.; Rosenberg, F. S. In *Better Ceramics Through Chemistry III*; Brinker, C. J.; Clark, D. E.; Ulrich, D. R., Eds.; Materials Research Society, Vol. 121; Elsevier Science Publishing Co., Inc.: New York, 1988; p 15.

(13) Kelts, L. W.; Amstrong, N. J. *J. Mater. Res.* **1989**, *4*, 423.

(14) Knight, C. T. G. Zeolites 1990, 10, 140.

(15) Brinker, C. J.; Scherer, G. W. *Sol−Gel Science: The Physics and Chemistry of Sol−Gel Processing*; Academic Press, Inc.: New York, 1989.

(16) Hench, L. L.; West, J. K. *Chem. Rev.* **1990**, *90*, 33.

(17) Sauer, J. *Chem. Rev.* **1989**, *89*, 199.

(18) Heanry, P. J.; Prewitt, C. T.; Gibbs, G. V. In *Silica, Physical Behavior, Geochemistry and Materials Applications*; Ribbe, P. H., Ed.; Reviews in Mineralogy, Vol. 29; Mineralogical Society of America: Washington, D.C., 1994; p 331.

(19) Gibbs, G. V.; Boisen, M. B. In *Better Ceramics Through Chemistry II*; Brinker, C. J.; Clark, D. E.; Ulrich, D. R., Eds.; Materials Research Society, Vol. 73; Elsevier Science Publishing Co., Inc.: New York, 1986; p 515.

(20) Hill, J.; Sauer, J. *J. Phys. Chem.* **1994**, *98*, 1238.

(21) Moravetski, V.; Hill, J.; Eichler, U.; Cheetham, A. K.; Sauer, J. *J. Am. Chem. Soc.* **1996**, *118*, 13015.

(22) Lasaga, A. C.; Gibbs, G. V. *Phys. Chem. Miner.* **1987**, *14*, 107.

(23) Lasaga, A. C.; Gibbs, G. V. *Am. J. Sci.* **1990**, *290*, 263.

(24) Pápai, I.; Goursot, A.; Fajula, F. *J. Phys. Chem.* **1994**, *98*, 4654.

(25) Gordon, M. S.; Pederson, L. A. *J. Phys. Chem.* **1990**, *94*, 5527.

(26) Ugliengo, P.; Saunders, V.; Garrone, E. *J. Phys. Chem.* **1990**, *94*, 2260.

(27) Bleiber, A.; Sauer, *Chem. Phys. Lett.* **1995**, *238*, 243.

(28) Ferrari, A. M.; Ugliengo, P.; Carrone, E. *J. Phys. Chem.* **1993**, *97*, 2671.

(29) Luke, B. T. *J. Phys. Chem.* **1993**, *97*, 7505.

(30) Stave, M. S.; Nicholas, J. B. *J. Phys. Chem.* **1993**, *97*, 9630.

(31) Mortier, W. J.; Sauer, J.; Lercher, J. A.; Noller, H. *J. Phys. Chem.* **1984**, *88*, 905.

(32) Brand, H. V.; Curtiss, L. A.; Iton, L. E. *J. Phys. Chem.* **1992**, *96*, 7725.

(33) Nicholas, J. B.; Winans, R. E.; Harrison, R. J.; Iton, L. E.; Curtis, L. A. *J. Phys. Chem.* **1992**, *96*, 10247.

(34) Bornhauser, P.; Calzaferri, *Spectrochim. Acta, Part A* **1990**, *46*, 7, 1045.

(35) Ahlrichs, R.; Bär, M.; Häser, M. *Chem. Phys. Lett.* **1989**, *164*, 2−3, 199.

(36) Andzelm, J.; Wimmer, E. *J. Chem. Phys.* **1992**, *96*, 2, 1280.

(37) Altmann, J. A.; Handy, N. C.; Ingamells, V. E. *Int. J. Quantum Chem.* **1996**, *57*, 4, 533.

(38) Limtrakul, J.; Tantanak, D. *J. Mol. Struct. THEOCHEM* **1995**, *358*, 179.

(39) *Dmol 96.0 Manual*; Molecular Simulations Inc.: San Diego, CA, 1996.

(40) Delley, B. *J. Chem. Phys.* **1990**, *92*, 1, 508.

(41) von Barth, U.; Hedin, L. *J. Phys. C.: Solid State Phys.* **1972**, *5*, 1629.

(42) Hedin, L.; Lundqvist, B. I. *J. Phys. C: Solid State Phys.* **1971**, *4*, 2064.

(43) Moruzzi, V. L.; Janak, J. F.; Schwarz, K. Calculated Thermal Properties of Metals. *Phys. Rev. B* **1988**, *37*, 2, 790.

(44) Becke, A. D. Density-Functional Exchange Energy Approximation with Correct Asymptotic Behavior. *Phys. Rev. A* **1988**, *38*, 6, 3098.

(45) Lee, C.; Yang, W.; Parr, R. G. Development of the Colle-Salvetti correlation energy formula into a functional of the electron density. *Phys. Rev. B* **1988**, *37*, 2, 785.

(46) *Discover 96.0 Manual*; Molecular Simulations Inc.: San Diego, CA, 1996.

(47) *Mopac 5.0 Manual*; University of Minnesota: Minneapolis, 1997.

(48) Baker, J.; Hehre, W. J. *J. Comput. Chem*. **1991**, *12*, 5, 606.

(49) Baker, J. *J. Comput. Chem.* **1993**, *14*, 9, 1085.

(50) Baker, J. *J. Comput. Chem.* **1986**, *7*, 4, 385.

(51) Baker, J. *J. Comput. Chem.* **1992**, *13*, 2, 240.

(52) Baker, J.; Bergeron, D. *J. Comput. Chem.* **1993**, *14*, 11, 1339.

(53) Amos, R. D.; Alberts, I. L.; Andrews, J. S.; Colwell, S. M.; Handy, N. C.; Jayatilaka, D.; Knowles, P. J.; Kobayashi, R.; Laidig, K. E.; Laming, G.; Lee, A. M.; Maslen, P. E.; Murray, C. W.; Rice, J. E.; Simandiras, E. D.; Stone, A. J.; Su, M.-D.; Tozer, D. J. *The Cambridge Analytic Derivatives Package; Cadpac 5.2 Manual.* University of Cambridge, 1995.

(54) Dunitz, J. D.; Ibers, J. A. *Perspectives in Structural Chemistry*; John Wiley & Sons, Inc.: New York, 1968; Vol. II.

(55) Pereira, J. C. G.; Catlow, C. R. A.; Price, G. D. *Chem. Commun*. **1998**, *13*, 1387.

(56) Stull, D. R. and Projhet, H., Eds. *Thermochemical Tables*, 2nd ed.; Joint Army-Navy-Air Force database, National Institute of Standards and Technology, Gaithersburg, MD, 1970.

(57) Kaye, G. W. C. and Laby, T. H., Eds.; *Tables of Physical and Chemical Constants*, 14th ed.; Longman: London, New York, 1973.

(58) Greenwood, N. N.; Garnshaw, A. *Chemistry of the Elements*; Pergamon Press: Elmsford, NY, 1984.

(59) Popkie, H.; Kistenmacher, H.; Clementi, E. *J. Chem. Phys.* **1973**, *59*, 3, 1325.

(60) Umeyama, H.; Morokuma, K. *J. Am. Chem. Soc.* **1977**, *99*, 5, 1316.

(61) Buther, I. S.; Harrod, J. F. *Inorganic Chemistry Principles and Applications*; The Benjamin Publishing Company: New York, 1989.

(62) Catlow, C. R. A.; George, A. R.; Pereira, J. C.; Coombes, D.; Freeman, C. M. Manuscript to be submitted for publication.

(63) Gale, J. D. *Top. Catalysis* **1996**, *3*, 1−2, 169.